CHEMICAL REVIEWS



Review

# Molecular Simulation of Water in Carbon Nanotubes

Alessio Alexiadis, and Stavros Kassinos

*Chem. Rev.*, **2008**, 108 (12), 5014-5034 • DOI: 10.1021/cr078140f • Publication Date (Web): 04 November 2008

# Molecular Simulation of Water in Carbon Nanotubes

Alessio Alexiadis and Stavros Kassinos*

*Computational Science Laboratory (UCY-CompSci), Department of Mechanical and Manufacturing Engineering, University of Cyprus, 75 Kallipoleos St., P.O. Box 20537, 1678 Nicosia, Cyprus*

*Received June 6, 2007*

## Contents



## 1. Introduction

According to Monthioux and Kuznetsov,[1] the first mention of carbon filaments was reported in 1889[2] in a patent proposing the use of such filaments in light bulbs (interestingly enough, the same idea was proposed again 115 years later[3]). Later, the existence of the *carbone filamenteux* was mentioned in two papers presented at the French Academy of Sciences.[4,5] These papers, however, did not provide evidence for the tubular nature of the filaments, since the resolution of the available microscopes was not high enough to reveal the inner cavity of the filament. In 1952, Radushkevich and Lukyanovich[6] published in the *Journal of Physical Chemistry of Russia* the first transmission electron microscopy (TEM) pictures showing the hollow structure of the carbon filaments. Western researchers, however, had limited access to the Russian press during the Cold War and the work of the two Soviet scientists remained basically unknown on the other side of the iron curtain. In 1991, carbon nanotubes (CNTs) were finally "rediscovered" by Sumio Iijima[7] and, this time, they immediately awakened the interest of the scientific community. Recently Monthioux and Kuznetsov[1] brought to light the work of Radushkevich and Lukyanovich, but the vast majority of academic and popular literature still attributes the discovery of the nanotubules of graphitic carbon to Iijima.

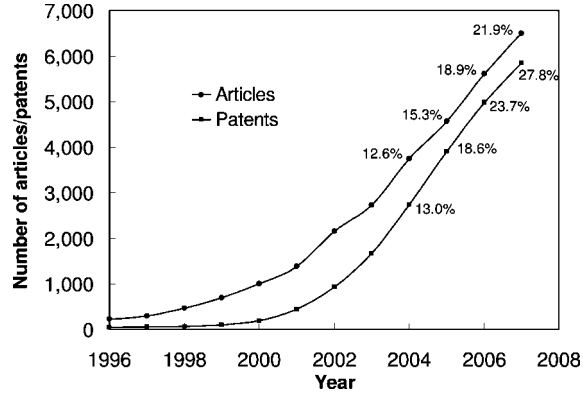


**Figure 1.** Number of articles/patents published/registered each year and having "nanotubes" as topic.

It must be said, however, that, apart from the attribution of their effective discovery, it was only after 1991 that the study of carbon nanotubes became one of the most active areas in microscopic physics. Furthermore, the existence of single-wall carbon nanotubes (SWNT) was actually discovered by Iijima[8] 2 years later (and by Bethune[9] at the same time).

From 1991 to 2007, according to the "Web of Science"[10] and Scopus[11] databases, CNTs appeared in more than 30 000 papers written by more than 37 000 authors and more than 20 000 patents. Figure 1 gives an idea of how the interest in this area, which supplanted fullerenes as the hottest research topic of the 20th century,[1,12] is growing year after year. The number of papers and patents is increasing exponentially; more than a fifth of all the papers and more than a quarter of the patents have been published or registered in 2007 and this trend seems to continue in 2008. To a large extent, this popularity is due to the remarkable structural, mechanical, and electromechanical properties[13,14] that make CNTs promising candidates for a large variety of applications such as gas storage,[15,16] nanoelectronics,[17,18] molecular detection,[19,20] membrane separation,[21,22] nanopipets,[23] nanotweezers,[24] nanopipes for the precise delivery of gases or liquids,[25,26] and drug delivery.[27,28] Certain experimental studies suggests that SWNTs can be internalized into living cells through endocytosis without apparent toxic effects[29,30] (this assessment, however, is under debate with some recent results

* Corresponding author. E-mail: kassinos@ucy.ac.cy. Tel.: +35722892296. Fax: +35722892254.

10.1021/cr078140f CCC: $71.00 
Published on Web 11/04/2008

Alessio Alexiadis graduated in chemical engineering in 1998 in Italy at the Politecnico di Torino. Three years later, he accomplished his Ph.D in the same institution with a thesis on photocatalytic reactors. Since then, he worked as a Postdoctoral Fellow in France at ARMINES Ecole Nationale Supérieuredes Mines de Paris (2001−2003), in Germany at Max-Planck-Institut für Kohlenforschung, Mülheim an der Ruhr (2003−2004), and in Australia at the UNESCO Centre for Membrane Science & Technology, University of New South Wales, Sydney (2004−2006). Currently, he works at the Computational Sciences Laboratory at the University of Cyprus (UCYCompSci). His research interests and activities include photocatalysis, bubbly flows, polymer dynamics, membrane science, global worming modeling, nanofluidics, and both classical and ab initio molecular simulations. He also collaborates with the Task Force on Plasma Wall Interaction of the ITER project.

Stavros C. Kassinos completed his undergraduate studies at the University of Texas at Austin (B.Sc. in Mechanical Engineering, 1986) while on a CASP/USIA scholarship. He followed with graduate studies in Mechanical Engineering at Stanford University in California (M.Sc. 1989, Ph.D. 1995). He continued to work in the Mechanical Engineering Department at Stanford University as a Postdoctoral Fellow till 1997, when he joined the Research Staff at the Stanford/NASA-Ames Center for Turbulence Research (CTR). Between 1999 and 2003 he also held a joint appointment at the Center for Integrated Turbulence Simulations (CITS) at Stanford University. He is currently an Associate Professor in the Department of Mechanical and Manufacturing Engineering at the University of Cyprus and the Head of the Computational Sciences Laboratory at the University of Cyrpus (UCY-CompSci) and of the Fusion Trasnational Unit for Research in Cyrpus (FUTURE-CY). His research interests center on the numerical simulation and modeling of complex physical systems and he has developed a particular interest in nanofluidic systems with biomedical and environmental applications. He teaches in the area of thermofluids and computational mechanics.

indicating that carbon nanotubes can be toxic[31]). As a molecular transporter, SWNTs can shuttle various cargoes across the cellular membrane, thus opening a new route for medicine delivery and giving rise to a novel mechanism for cancer therapy.[32] Central to many of these applications is the capacity to store or convey fluids, and in particular aqueous solutions, at nanoscale precision. For this reason, the study of CNT/water systems is of paramount importance for the development and evolution of the related technologies. However, even if CNTs end up having no practical applications, as it happened, for instance, with fullerenes, whose commercial applications remain limited despite all initial expectations, the study of water confinement in CNTs would still maintain a high theoretical importance to chemistry, biology, and materials science.[33,34] In fact, water-filled and water-permeable pores are present in biological cells, membranes, and surface of proteins[35] and in other relevant biological and geological (e.g., zeolites[36]) systems that may present a strict analogy with water confined in carbon nanotubes.[37] For all these reasons, the mathematical modeling of the flow of fluids, and in particular of water, through carbon nanotubes has increasingly attracted the interest of researchers in the last years. Molecular dynamics (MD), which can be as accurate as experiments and much easier to perform at the nanoscale, has proven to be the most natural and flexible tool for this kind of analysis. The first paper dealing with MD simulation of water in CNTs was published in 2000[38] and it was immediately followed by many others, which in a few years accumulated a large amount of information. The aim of this review is to summarize the recent advances, to highlight the controversial issues, to provide, in some cases, practical correlations based on the available data and, hopefully, to give a starting point for the researchers who approach this topic for the first time.

## 2. Molecular Dynamics

Molecular dynamics is a form of investigation where the motion and the interaction of a certain number of "virtual" atoms or molecules are studied. Today, it is automatically assumed that these virtual representations are numerical and their evolution is calculated in the microchips of a computer. Early MD, however, involved "physical" substitutes of atoms like steel spheres,[39] seeds,[40] or gelatin balls.[41] These attempts gave relatively good results but were limited by the concrete difficulty of handling a large number of physical objects and by the presence of gravity. The natural evolution of this approach, therefore, was to use mathematical rather than physical "objects" and to calculate their motion through numerical procedures. The first computer code envisaged for this task was made in 1953 by M. Tsingou and, although she does not appear in the list of authors, it was used to carry out the calculations of the celebrated Fermi−Pasta−Ulam paper.[42] Since then, the theory and the application of MD have developed quickly, driven by advances both in numerical techniques and in computer hardware. The method gained popularity in many areas of research such as materials science, biochemistry, or biophysics, but probably the marriage with nanotechnology is the most promising of all. In fact, typical MD simulations can be performed on systems containing thousands or, perhaps, millions of atoms and for simulation times ranging from a few picoseconds to hundreds of nanoseconds. These values are certainly respectable, but the number of atoms contained in a typical macroscopic system is of the order of $10^{23}$, which is still beyond the possibilities of modern supercomputers. At the nanoscale, however, the amount of atoms is much smaller and sometimes MD can handle the exact number of atoms contained in the system under study. Moreover, at the moment the practical possibility of manipulating real objects at the nanometer scale is still limited and MD can be used to

**Table 1. Comparison between CHARMM and AMBER Values for C−C Intramolecular Interaction (Eqs 5 and 6 and 7)[a]**

| force field | $k_{stretch}$ (kcal mol$^{-1}$ Å$^{-2}$) | $r_0$ (Å) | $k_{angle}$ (kcal mol$^{-1}$ rad$^{-2}$) | $\theta_0$ (deg) | $k_{dihedral}$ (kcal mol$^{-1}$) | $n$ | $\phi_0$ (deg) | $\sigma_{C-C}$ (Å) | $\epsilon_{C-C}$ (kcal mol$^{-1}$) |
|---|---|---|---|---|---|---|---|---|---|
| CHARMM | 305 | 1.375 | 40 | 120 | 3.1 | 2 | 180 | 3.55 | 0.070 |
| AMBER | 469 | 1.4 | 63 | 120 | 3.625 | 2 | 180 | 3.4 | 0.086 |

[a] $k_{stretch}$ and $r_0$ are respectively the stretch constant and the equilibrium distance in eq 5, $k_{angle}$ and $\theta_0$ are the angle-stretching constant and equilibrium angle in eq 6, $k_{dihedral}$, $n$, and $\phi_0$ are the constant and the parameters of eq 7, while $\sigma_{C-C}$ and $\epsilon_{C-C}$ are the Lennard-Jones parameters for the carbon−carbon interaction.

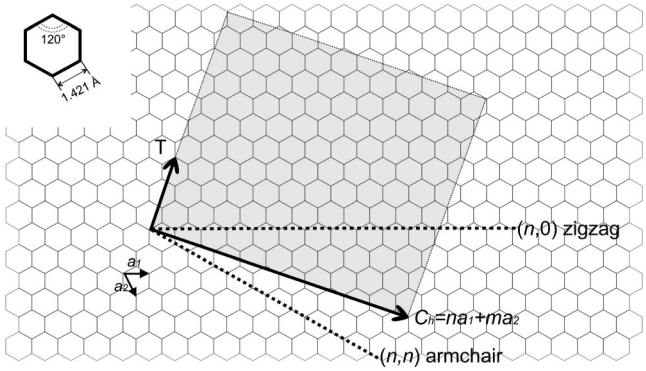


**Figure 2.** Graphene sheet, $\vec{T}$ and $\vec{C}_h$ vectors. In order to obtain the nanotube, imagine cutting the gray area and rolling it along the $\vec{T}$ vector in such a way that $C_h$ gives the final circumference of the CNT.

examine nanodevices that have not or cannot yet be created. This circumstance could play a major role in the near future since a rush to secure the highest number of patents and gain an advantage in the forthcoming "nanorevolution" is under way all around the world.[43]

The concrete difficulties of handling nano-objects involve also experiments. In fact, presently, experimental investigation of many nanoscale systems faces problems due to a certain lack of imaging tools: the nanoscale is too small for light microscopy and too large for X-ray crystallography; in certain cases it is too heterogeneous for NMR and, in others, too "wet" for electron microscopy.[37] Computer simulations, on the other hand, provide an excellent research tool, dealing quite well with the length and time scales under consideration. The simulation of carbon nanotubes interacting with biomolecules, in particular, has reached such close agreement with observation that today more and more researchers have begun to rely on this methodology in their design strategies.[37]

The reader interested in the theory and the computational methods of (classical) molecular dynamics can find additional information in several books that are routinely used for learning these topics.[44−48]

## 3. Molecular Dynamics Force Fields

In classical MD simulations atoms move according to the Newtonian equations of motion

$$m_i \frac{\partial^2 \vec{r}_i}{\partial t^2} = -\frac{\partial}{\partial \vec{r}_i} U_{tot}(\vec{r}_1, \vec{r}_2, ..., \vec{r}_N), \quad i = 1, 2, ..., N \tag{1}$$

where $m_i$ is the mass of atom $i$, $r_i$ is its position, and $U_{tot}$ is the total potential energy that depends on all atomic positions. The potential energy is the most crucial part of the simulation because it must faithfully represent the interaction between atoms in the form of a simple mathematical function that can be calculated quickly by a computer. Some of the most widely known MD software are based on certain force-field packages like AMBER,[49] GROMACS,[50] CHARMM,[51] OPLS,[52] MM3,[53] MM4,[54] DREIDING,[55] AMOEBA,[56] and many others,[57,58] which have been studied and tested for certain typical applications. Conceptually, the forces acting on atoms are divided into nonbonded and intramolecular atomic forces.

### Nonbonded Atom Forces

Atoms can interact through electrostatic forces, attractive forces at long ranges (van der Waals force) and repulsive forces at short ranges (the result of overlapping electron orbitals) referred to as Pauli repulsion.

The Lennard-Jones potential[59] (also referred to as the L-J potential or 6−12 potential) is a simple mathematical model, which combines together van der Waals attraction and Pauli repulsion

$$U_{vdW}(r_{i,j}) = 4\epsilon_{i,j}\left[\left(\frac{\sigma_{i,j}}{r_{i,j}}\right)^{12} - \left(\frac{\sigma_{i,j}}{r_{i,j}}\right)^{6}\right] \tag{2}$$

where $\epsilon$ is the depth of the potential well and $\sigma$ is the (finite) distance at which the potential is zero. Due to its simplicity, this potential is by far the most common in MD simulations of CNTs and water. The fast decay of the Lennard-Jones potential usually allows a truncation of the potential at a certain cutoff distance $r_c$. Typical values of $r_c$ in water/CNT simulations are between 9 and 10 Å. Banerjee et al.[60] carried out a sensitivity analysis verifying that results were insensitive to cutoff radii greater than 9.5 Å.

The electrostatic potential follows the known Coulomb law

$$U_{coulomb}(r_{i,j}) = \frac{q_i q_j}{4\pi\epsilon_0 r_{i,j}} \tag{3}$$

where $q_i$ and $q_j$ are the electrostatic charges of atom $i$ and $j$, $r_{i,j}$ is the distance between them, and $\epsilon_0$ is the dielectric constant. The decay of the electrostatic potential is not as sharp as in the previous case and can create certain problems especially in connection with periodic boundary conditions. In order to tackle this problem, specific summation techniques such as the Ewald summation[61] or the particle-mesh Ewald summation[62] have been developed over the years.

### Intramolecular Forces

The modeling of intramolecular forces presents a larger variety of cases and different kinds of potentials. An expression, which is often used by MD software like AMBER,[49] GROMACS,[50] CHARMM,[51] or NAMD[63] is based on the following approximation.

$$U_{intramolecular} = U_{stretch} + U_{angle} + U_{dihedral} \tag{4}$$

Each contribution to $U_{intramolecular}$ can be further modeled by the following equations

$$U_{\text{stretch}} = k_{\text{bond}}(r - r_0)^2 \quad (5)$$

$$U_{\text{angle}} = k_{\text{angle}}(\theta - \theta_0)^2 \quad (6)$$

$$U_{\text{dihedral}} = k_{\text{dihedral}}(1 + \cos(n\phi - \phi_0))^2 \quad (7)$$

$U_{\text{stretch}}$ models the potential exerted when the bond is stretched from its initial position $r_0$ to the new position $r$; $U_{\text{angle}}$ models the potential exerted when the angle $\theta$ between two bonds changes with respect to its initial angle $\theta_0$; $U_{\text{dihedral}}$ describes the potential that atoms separated by three covalent bonds exert when they are subject to a torsion angle $\phi$.[63] An improper dihedral potential, which regards three planar atom bonds, also exists but it is not reported here because such a possibility does not appear either in water or in CNTs. As an example of the values that these parameters can assume in the case of C−C bonds in CNTs, see Table 1. The potentials expressions reported in this section have been used for MD simulation of water in CNT. They do not, however, exhaust all the possibilities; other intramolecular potentials, and in particular the Brenner empirical potential for C−C bonds in a nanotube, are sometimes used. These potentials regard specifically the CNT and are mentioned in the next section.

In the case of ab initio molecular dynamics simulations, finally, the forces experienced by the atoms are not computed from empirical interatomic potentials, but from quantum-mechanical calculations updated at each time step. The core of these methods, as a consequence, lies in the scheme used to approximate the Schrödinger equation.[64−66] Ab initio calculations produce a large amount of information that is not available from classical MD, at the cost, however, of very long computational times, which, at the moment, limit the use of this method to maximum of a few thousands particles.

## Thermostats and Barostats

In order to perform MD simulations in the canonical (NVT) or in the isothermal−isobaric (NPT) ensemble, the system may be coupled to a thermostat, which ensures that the average temperature is maintained close to a certain value, or to a barostat, which adjusts the size and shape of the simulation cell in order to maintain the desired average pressure. There are many methods (e.g., the Berendsen[67] and Nosé−Hoover[68,69] thermostats or the Berendsen[67] and Parrinello−Rahman[70] barostats) designed to accomplish in a realistic way this task. These methods, however, can sometimes artificially affect the final results of the simulation. In the specific case of CNTs, for instance, Heo and Sinnot[71] showed that the calculated mechanical properties of SWNTs are influenced by the choice of the thermostat and not all of them are suitable for this kind of simulations. As it will be explained later, it is not completely clear what effect different thermostats and barostats can have on the arrangement of $H_2O$ molecules in CNTs and, probably, more investigation in this direction is required.

## 4. Some Properties of Carbon Nanotubes

Carbon nanotubes (CNTs), together with graphite, diamond, fullerenes, and other more exotic structures like carbon nanohorns,[72] are allotropes of carbon. They are commonly formed in ordinary flames, produced by burning methane,[73] ethylene,[74] or benzene,[75] and they have been found in soot from both indoor and outdoor air.[76] However, these naturally occurring varieties are highly irregular in size and quality and thus, for commercial purposes, they are usually produced by other means like arc discharge,[77] laser ablation,[78] or chemical vapor deposition.[79] During CNTs synthesis, many impurities in the form of catalyst particles, amorphous carbon, and nontubular fullerenes are also produced. Subsequent purification steps are thus required to separate the tubes from these undesirable byproducts. Moreover, SWNTs are often produced with closed ends[80] and they must be heated for a certain time above 700 °C in order to burn away the tips and obtain open nanotubes. All these processes make carbon nanotubes rather expensive, up to 1300 euros/g (this price refers to high-purity, >90%, single-wall carbon nanotubes produced with the arc discharge method, with diameter between 1 and 1.5 nm and length >10 $\mu$m in April 2008), and the reduction of their price is one of the goals of the near future. After relatively high quantities of CNTs were recently discovered in ancient damascus sabres,[81] it has been suggested that the method involved in forging damascus steel (a forging technique lost to time), if rediscovered, may provide important information for manufacturing cheap nanotubes.

There are two main types of CNTs: multiwalled nanotubes (MWNTs) and single-walled nanotubes (SWNTs). The latter are probably more important in nanotechnology, although recently double-walled carbon nanotubes (DWNT)[82] have attracted interest due to their properties, which are similar to SWNT, but with significantly higher resistance to chemicals (this could play an important role in the area of functionalized nanotubes). A single-wall carbon nanotube is a one-atom-thick sheet of graphite (called graphene) rolled up into a seamless cylinder. In order to obtain the nanotube, imagine cutting the gray area in Figure 2 and rolling it along the $\vec{T}$ vector in such a way that $\vec{C}_h$ gives the final circumference of the CNT. The way the graphene sheet is wrapped is represented by a pair of indices $(n,m)$, which determine the so-called chiral vector. The integers $n$ and $m$ denote the number of unit vectors along two directions $\vec{a}_1$ and $\vec{a}_2$ (Figure 2) in the honeycomb crystal lattice of graphene. If $m = 0$, the nanotubes are called *zigzag*. If $n = m$, they are called *armchair*. Otherwise, they are called *chiral* (or *helical*) nanotubes (this classification refers to the rim nanotube structure). The diameter of the tube is given by

$$d_{\text{CNT}} = \frac{\sqrt{3}(n^2 + m^2 + nm)^{1/2}}{\pi} a \quad (8)$$

where $a = 1.421$ Å is the distance between two carbon atoms.

The chiral angle is given by

$$\vartheta = \arctan\left(\frac{\sqrt{3}m}{m + 2n}\right) \quad (9)$$

The vector $\vec{T} = t_1\vec{a}_1 + t_2\vec{a}_2$ gives the unit cell of the nanotube. It can be described by a pair of integers $(t_1, t_2)$ related to the chiral indices via

$$t_1 = \frac{2m + n}{d_R} \quad (10)$$

and

$$t_2 = -\frac{2n + m}{d_R} \quad (11)$$

where $d_R$ is the greatest common divisor of $(2n + m, 2m + n)$.

The length of the vector $\vec{T}$ is given by

$$|\vec{T}| = \frac{\sqrt{3}\pi d_{CNT}}{d_R} \quad (12)$$

and the number of atoms per unit cell of the nanotube is

$$n_c = \frac{4(n^2 + m^2 + nm)}{d_R} \quad (13)$$

The above expressions[83] assume that the process of wrapping the graphene sheet into a cylindrical tube does not distort the relative distance $a$ and the 120° angle between two carbon atoms. This is not true, however, for very small diameter nanotubes ($d_{CNT} < 1$ nm), where the curvature causes the bond angles to deviate below the ideal 120°.

The chemical bonding of nanotubes is composed entirely of sp2 bonds, similar to those of graphite. This bonding structure, which is stronger than the sp3 bonds found in diamond, provides the molecules with their unique strength. The chirality, on the other hand, affects the electric properties of CNTs. It is commonly assumed that, if $n - m$ is a multiple of 3, then the nanotube is metallic, otherwise the nanotube is a semiconductor. More recent studies[84] classify electronic characteristics of SWNTs in eight categories, which include four metallic and four semiconductor types.

### 4.1. Molecular Dynamics of Empty Carbon Nanotubes

Many MD studies have been carried out in order to determine some of the mechanical properties of CNTs (e.g., Young modulus and tensile strength,[85] radial compression and deformation,[86] fracture behavior,[87] radial breathing mode,[88] torsional deformation,[89] etc.). Comparison between various theoretical predictions and experimental measurements available in literature was performed in Ruoff et al.[90] The results are usually of the same order of magnitude, although experiments can be affected by the presence of defects (e.g., atomic vacancies) in the nanotube structure. These studies are focused on the nanotube itself and they do not consider interaction with water or any other substance.

The harmonic approximation of the intramolecular potential (eqs 5, 6, and 7) is acceptable when the bond deformation is not particularly high, but other functions must be used in order to take into account more extreme conditions. The empirical potential of Tersoff[91] in the form suggested for carbon by Brenner,[92] in particular, has been widely used.[85,93,94] More recently, a new version of this potential, called second-generation reactive empirical bond order (REBO), was proposed and used in modeling many different physical properties of carbon nanotubes.[88,95−97] It must be stressed, however, that these works studied the CNT under conditions that cause very high deformation of the C−C bonds. The deformation taken into account in papers that studied CNTs in water, however, is not particularly high and the majority of works considered the nanotube to be rigid or, occasionally,[98,99] flexible with harmonic potentials (eqs 5, 6, and 7). The Morse potential for $U_{stretch}$ was rarely employed,[100] while the Brenner or REBO potentials in the case of water in CNTs, to our knowledge, were used only in the works of Longhurst and Quirke[101−103] (the Brenner potential was also used in Zhou et al.,[99] but only during the equilibration phase). Probably differences resulting from using either of these potentials are not significant because of the small bond deformation. At the moment, however, a systematic study comparing the consequences of using different C−C intramolecular potentials in water/CNT simulations is not available in the literature. In Alexiadis and Kassinos,[104,105] however, calculations carried out with rigid and flexible (harmonic potential) CNTs in water show that the C−C bond deformations are small (order of magnitude 0.01 Å) and that certain water properties (density, self-diffusivity, and hydrogen bonding) exhibit similar values in rigid or flexible CNTs. Other properties, however, seem to depend on the nanotube flexibility. Andrev et al.,[106] for instance, found that flexibility increases the effective hydrophobicity of the nanotube with consequences on the filling dynamic of CNTs in water.

## 5. Water Models

Water is the most studied material on earth, but some of its characteristics and properties are still not completely understood. This depends on the fact that water has some unique features which make it an incredibly anomalous substance (63 anomalies and other remarkable properties of water have been listed in a recent online review[107]). A large number of "hypothetical" models for water have been proposed during the years. Generally, each model is developed to fit well one particular physical characteristic of water (e.g., density, radial distribution, or critical parameters) at the expenses of others. A recent review listed 46 distinct models,[108] a fact that indirectly indicates the lack of success in quantitatively reproducing all the properties of real water. Furthermore, all these models were proposed for simulating, with classical MD calculation, the behavior of bulk water. As a consequence, there is a certain contradiction in using them in the case of confined water where they are not validated. Inside nanotubes, in fact, $H_2O$ molecules have a different arrangement and the respective electronic clouds differ from those of bulk. This makes, at least in theory, the empirical potentials and, consequently, all the models inadequate for confined water. Strictly speaking, the correct solution should require ab initio simulations instead of classical. This type of simulations, however, are computationally much more expensive and, with a few exceptions concerning only small CNTs,[109,110] they have been not carried out. It is likely, however, that the simulation of CNTs of average size (10−15 Å) will soon become more affordable since the computer power is continuously increasing year after year. These considerations make the choice of the water model critical, since there are no means to conclude that a particular model is more reliable than others, at least until adequate experimental or ab initio analysis is available. For this reason, at this stage, the best practice for classic MD simulations of water in CNTs is probably to compare the results obtained with different models.[104,105] In Table 2, the most frequently used water models for MD in CNT are listed; $\sigma$ and $\epsilon$ are the Lennard-Jones parameters for the O−O interaction, while the H−H interactions are often neglected (those interactions are not really neglected as there is a Coulombic interaction between the H and O atoms; water hydrogens are represented as point charges without any corresponding Lennard-Jones force but the rest of the force field is parametrized in order to compensate). The charge distribution of water molecules is modeled by point charges on the nuclei. In the case of the TIP4P and TTM2-F models, however, the negative charge is placed on an additional fictive site (Figure 3) located at a certain distance $r_1$ from

**Table 2. Water Models Parameters**[a]

| model | $\sigma_{O-O}$ (Å) | $\epsilon_{O-O}$ (kJ mol$^{-1}$) | $r_0$ ($r_1$) (Å) | $q_1$ (e) | $q_0$ (e) | $\theta_{0(1)}$ ($\theta_1$) (deg) |
|---|---|---|---|---|---|---|
| SPC[209] | 3.166 | 0.650 | 1.0 | +0.41 | −0.82 | 109.47 |
| SPC/E[210] | 3.166 | 0.650 | 1.0 | +0.4238 | −0.8476 | 109.47 |
| TIP3P[211] | 3.15061 | 0.6364 | 0.9572 | +0.4170 | −0.8340 | 104.52 |
| TIP4P[212] | 3.15365 | 0.6480 | 0.9572 (0.15) | +0.52 | −1.04 | 104.52 (52.26) |
| TTM2-F[112] | n.a. | n.a. | 0.9572 (0.7) | +0.574 | −1.148 | 104.52 (52.26) |

[a] $\sigma_{O-O}$ and $\epsilon_{O-O}$ are the Lennard-Jones parameters for the oxygen−oxygen interaction, $r_0$ is the O−H distance, $q_1$ and $q_0$ are the partial charges located respectively on the hydrogens and the oxygen (or the fourth site), and $\theta_0$ is the H−O−H angle. The values between parentheses refer to the distance ($r_1$) and angle ($\theta_1$) of the additional site in the four-sites models (TIP4P and TTM2-F). See also Figure 3.

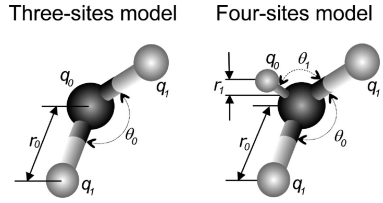


**Figure 3.** Schematic representation of three-site and four-site water models. See Table 2 for the meaning of the various parameters.

the oxygen nuclei. SPC, SPCE, and TIP3P are thus defined three-site models, while the TIP4P and TTM2-F are four-site models. There are flexible versions of these models, where the bond distances and angles between atoms can vary according to harmonic laws (eqs 5 and 6). The SPC(flex),[111] for instance, is equivalent to the SPC model with $k_{bond} = 4637$ kJ mol$^{-1}$ Å$^{-2}$ (see eq 5) and $k_{angle} = 383$ kJ mol$^{-1}$ rad$^{-2}$ (see eq 6). The TTM2-F model is a polarizable model, where induced dipoles are placed on the atoms.[112] This model, furthermore, does not use the Lennard-Jones equation, but the following five parameter expression.

$$U_{vdW} = \frac{A}{r^{12}} + \frac{B}{r^{10}} + \frac{C}{r^6} + De^{-Er} \tag{14}$$

with $A = -1\,329\,565.985$ Å$^{12}$ kcal/mol, $B = 363\,256.0798$ Å$^{10}$ kcal/mol, $C = -2147.141\,323$ Å$^6$ kcal/mol, $D = 10^{13}$ kcal/mol, and $E = 13.2$ Å$^{-1}$.

Five- and six-site models are also available in the literature, but these models have not been used so far in CNT/$H_2O$ simulations and they are not considered here. Table 3 compares some (bulk) experimental water properties with results calculated with different models. The effect of different models on certain water parameters such as density, hydrogen bonding or self-diffusivity of water in CNTs was studied in Alexiadis and Kassinos.[105] The results show that the property more affected by the choice of water model is the self-diffusivity. The same happens, however, also in the case of bulk water.

## 6. Carbon−Water Interaction

The choice of carbon−oxygen parameters is crucial to the calculated behavior of confined water. Hummer et al.[98] found that a minute reduction in the attraction between carbon and oxygen could lead to consistent differences in the results. Often the values of the C−O interaction are calculated according to the Lorentz−Berthelot rule

$$\sigma_{C-O} = \frac{1}{2}(\sigma_C + \sigma_O) \tag{15}$$

and

$$\epsilon_{C-O} = (\epsilon_C \epsilon_O)^{1/2} \tag{16}$$

The values of $\sigma_O$ and $\epsilon_O$ come from the water model, while those of $\sigma_C$ and $\epsilon_C$come from the force field. Therefore, many values of $\sigma_{C-O}$ and $\epsilon_{C-O}$, coming from many different combinations of water models and force fields, can be derived. Alternate values, not calculable from the Lorentz−Berthelot rule, have also been used. In certain cases,[113−115] the old parameters proposed by Bojan and Steele[116] ($\sigma_{C-O} = 0.319$ Å and $\epsilon_{C-O} = 0.3126$ kJ/mol) were used. These values, however, were calculated not for $H_2O$ but for $O_2$ absorption. Werder et al.[117] discussed the influences of the C−O interaction on the contact angle of a water droplet on graphite and proposed a new pair of parameters which could reproduce real macroscopic contact angles ($\sigma_{C-O} = 0.319$ Å and $\epsilon_{C-O} = 0.3920$ kJ/mol). According to Wang et al.,[118] however, these values may be only suitable for very large CNTs, while for smaller diameters AMBER parameters used by Hummer et al.[98] can reproduce, to some extent, experimental results.[22] The question is still open and, probably, it will not be resolved until a larger amount of ab initio simulations will be available. There is, however, the possibility that universal values of the mixing C−O parameters cannot be found and their optimal value depends on the CNT size. This case would mean that, at least in theory, the L-J approximation of the potential is not completely correct in the case of water−CNTs systems.

### 6.1. Contact Angle

The contact angle is a property of water and, strictly speaking, it should be presented in section 8, where we discuss the properties of water in carbon nanotubes. However, it is taken into consideration here since it has a close connection with the identification of the carbon−water interactions considered in the previous section. In fact, the most commonly used C−O parameters, explicitly defined for CNT−water systems, were calibrated in order to reproduce the contact angle of water on graphitic surfaces.[117,119]

First, it must be noted that the notion of contact angle is a macroscopic concept and it is not fully applicable to the nanometer scale. For this reason, Nijmeijer et al.[120] conceived a technique to visually determine the contact angle of a fluid between two walls, which can be used for analyzing MD results. Second, it is a known result that the surface of graphite is hydrophobic and the contact angle of water on graphite is 80°−90°.[121] This observation, nevertheless, does not automatically imply that, at the nanoscale, drops of water within nanotubes conserve the same behavior. For example, the measured contact angle of liquid drops on a smooth surface, like a graphene sheet, appears to decrease as the size of the drop decreases.[122] For this reason, Werder et al.[123,124] investigated the possibility that water inside CNTs could show hydrophilic instead of hydrophobic behavior. Their results indicated that the contact angle depends on the drop size, but it is always higher than 100°. This, however, contradicts experiments[125] that show wetting behavior of water in CNTs. Werder et al.,[117] later, gave a possible

**Table 3. Comparison between Water Experimental Properties and Calculated Using Different Models**

| model | dipole moment (D) | dielectric const (−) | self-diffusion ($10^{-5}$cm$^2$ s$^{-1}$) | density max (°C) | expansion coeff ($10^{-4}$ °C$^{-1}$) |
|---|---|---|---|---|---|
| SPC | 2.27[213] | 65[214] | 3.85[215] | −45[216] | 7.3[217] |
| SPC/E | 2.35[218] | 71[218] | 2.49[215] | −38[219] | 5.14[217] |
| TIP3P | 2.35[212] | 82[218] | 5.19[215] | −91[216] | 9.2[212] |
| TIP4P | 2.18[212] | 53[218] | 3.9[215] | −25[215] | 4.4[212] |
| TTM2-F | 2.67[112] | 67.2[112] | 1.4[112] | − | − |
| expt | 2.95[220] | 78.4 | 2.3 | +3.9 | 2.53 |

explanation of this inconsistency. The contact angle, in fact, was found to depend strongly on the C−O interaction and in particular on $\epsilon_{C-O}$. By increasing this parameter, the C−O binding energy decreases (the interaction force, consequently, increases) and, below a certain threshold (−12.82 kJ mol$^{-1}$), the droplet completely spreads on the graphitic surface. Thus, Werder et al.[117] considered the hypothesis that the nanotubes used in the aforementioned experiments could have numerous defects and/or attached hydroxyl or carboxyl groups, which would modify the water−CNT interaction.

When we take into consideration droplets at the macroscale, there is an additional interesting aspect which deserves to be mentioned. It turns out that materials coated with carbon nanotubes can show very different wetting behaviors according to the surface arrangement of the nanotubes.[126] A dense, vertically aligned carbon nanotubes distribution (sometimes called CNT forest[127]), for instance, can show stable superhydrophobic properties with a contact angle >150°. As a consequence, spherical, micrometer-sized water droplets can be suspended on top of the nanotube forest and exhibit the so-called "lotus effect". The lotus effect is the property of certain superhydrophobic substances of self-cleaning themselves. In this case, water droplets do not adhere to the material but roll away, picking up, during this process, any sort of dirt accumulated to the surface. The name comes from the fact that, although lotuses grow in muddy lakes or rivers, their (superhydrophobic) leaves remain clean. For this property, the lotus plant is, in some cultures, a symbol of purity.[128]

## 7. Water Confined in Carbon Nanotubes: General Overview

The Navier−Stokes equation can provide a reasonable description of fluids hydrodynamics only at very small Knudsen numbers.[129] When the system length scale reduces to the nanometer, however, the behavior of the flow is mainly affected by the movements of the discrete particles that compose the system at atomic level. At this scale, MD becomes the most effective way to describe the details of the flow and to study many fundamental nanofluid problems, which can be extremely difficult to investigate by other means. In the specific field of fluids confined in nanotubes, early works were focused on the behavior of simpler fluids like methane,[130,131] ethane,[130] ethylene,[130] argon,[132,133] helium,[133] neon,[132] and hydrogen[16,33] or water confined in simpler nanopores.[34,134−137] The first article, to our knowledge, dedicated to MD of water in CNTs was written by Gordillo and Martì[38] and followed by many others. These works can be divided into different categories according to the force field and the water model used, the $T$ and $P$ conditions, and the dimension of the nanotubes investigated. It is commonly assumed that the behavior of many properties of water in CNTs depends on the diameter of the nanotube, but not on its chirality. It must be noted, however, that in the majority of cases only armchair ($n$,$n$), less frequently zigzag ($n$,0), and only rarely chiral ($n$,$m$) nanotubes were investigated. The vast majority of articles use classical MD; there are, however, a few works based on ab initio MD simulation.[109,110] These studies have focused on small CNTs like (6,6) since ab initio simulations are computationally much more expensive than classic MD. A general overview of the simulations available in the literature is reported in Tables 4 and 5. In the majority of cases, the simulations were carried out in the canonical ensemble and only rarely in the isothermal−isobaric ensemble (in Table 5 where the pressure is not specified). Finally, Zheng et al.[138] and Striolo et al.[139−141] ran their simulation in the grand canonical ensemble.

The effects of confinement within CNTs on some of the chemical−physical properties of water like structure, density, H-bonds, dipole orientation, proton transport, etc., are illustrated in detail in the following sections.

### 7.1. Water Structure in Carbon Nanotubes

We are so used to dealing with water in our everyday life that it is difficult to believe how differently this substance can behave in confined nanospace. If the diameter of the nanotube is comparable to the size of $H_2O$ molecules, in fact, water molecules inside the CNT cannot cross each other and they can only move as a single file (Figure 4). The structure of water in larger CNTs, on the other hand, shows a typical layered structure, which covers the internal walls of the nanotube. The molecular arrangement within these layers, however, varies from work to work. Noon et al.[142] and Liu et al.[143,144] found that the molecules are arranged in a very ordered fashion, where the water layers are twisted forming a spiral-like chain of water molecules along the CNT axis (see Figure 5). Koga et al.,[145] on the other hand, found that water at very high pressure (500−5000 bar) could form $n$-gonal rings. The value of $n$ was found to depend on the nanotube diameter with $n = 4$ in the case of (14,14), $n = 5$ in case of (15,15), and $n = 6$ in the case of (16,16) (Figure 6 shows the case of $n = 6$). The structure is relatively stable and only rarely a "defect" is observed. Usually the defect is quickly reabsorbed, but if the diameter is increased, the lifetime of the defects increases until they gradually destroy the ordered structures. Mashl et al.[146] observed the same structure with $n = 6$ inside a (9,9) CNT at ambient conditions, but they did not find any similar arrangement within (7,7), (8,8), or (10,10) tubes. The (10,10) nanotube was also investigated by Kolesnikov et al.,[114] who found an octagonal water-shell structure with an additional central water chain inside the CNT. The same research group[113] later investigated smaller (9,9) nanotubes and found a structure having only the octagonal shell. A similar structure was also found by de Souza et al.,[147] who calculated that the water molecules' fluctuations increase drastically with temperature, leading to the disappearance of the ordered structure at ∼210

**Table 4. General Overview of $H_2O$/CNT Simulations (First Part)[a]**

| | ref | water model | force field | software | CNT |
|---|---|---|---|---|---|
| 1 | Gordillo and Martì (2000)[38] | SPC (flex) | 221 | ns | R |
| 2 | Hummer et al. (2001)[98] | TIP3P | AMBER | AMBER | F |
| 3 | Koga et al. (2001)[145] | TIP4P | 222 | ns | R |
| 4 | Noon et al. (2002)[142] | TIP3P | CHARMM | CHARMM | R |
| 5 | Werder et al. (2001)[123] | SPC (flex) | 116 | ns | F |
| 6 | Waghe et al. (2002)[167] | SPC | AMBER | AMBER | R |
| 7 | Mashl et al. (2003)[146] | SPC/E | GROMOS | GROMACS | R |
| 8 | Kalra et al. (2003)[22] | TIP3P | AMBER | AMBER | R |
| 9 | Dellago et al. (2003)[109] | ab initio | ab initio | ns | F |
| 10 | Mann and Halls (2003)[110] | ab initio | ab initio | VASP | F |
| 11 | Zhu and Schulten (2003)[172] | TIP3P | CHARMM | NAMD | R |
| 12 | Kolesnikov et al. (2004)[114] | TTM2-F | 116 | ns | R |
| 13 | Wang et al. (2004)[118] | TIP3P | AMBER | DL_POLY | R |
| 14 | Kassinos et al. (2004)[188] | SPC (flex) | 117 | FAST_TUBE | R |
| 15 | Kotsalis et al. (2004)[189] | SPC/E | 117 | FAST_TUBE | R |
| 16 | Huang et al. (2004)(5)[192,223] | TIP3P | CHARMM | CHARMM | F |
| 17 | Moulin et al. (2005)[200] | TIP4P | 221 | ns | R |
| 18 | Wan et al. (2005)[224] | TIP3P | AMBER | GROMACS | F |
| 19 | Liu et al. (2005)[143,144,157] | SPC | 15 | THINKER | R |
| 20 | Zheng et al. (2005)[138] | SPC | OPLS | ns | R |
| 21 | Zimmerli et al. (2005)[173] | SPC/E | 117 | ns | R |
| 22 | Striolo et al. (2005)(6)[139−141] | SPC/E | 222 | DL_POLY | R |
| 23 | Kotsalis et al. (2005)[225] | SPC/E | 117 | ns | R |
| 24 | Li et al. (2006)[226] | TIP4P | 117 | Lucretius | R |
| 25 | Hanasaki et al. (2006)[161−163,227] | SPC/E | 117 | ns | R |
| 26 | Huang et al. (2006)[156,208] | SPC/E | OPLS-AA | THINKER | R |
| 27 | Won et al.[201] | SPC/E | 197 | GROMACS | R |
| 28 | Zou et al.[100] | TIP3P | AMBER | GROMACS | F |
| 29 | de Souza et al. (2006)[147] | TTM2-F | 116 | ns | R |
| 30 | Takaiwa and al. (2007)[148] | TIP4P | 222 | ns | R |
| 31 | Zhou and Lu (2007)[99] | TIP3P | ns | AMBER | F |
| 32 | Mukherjee et al. (2007)[183] | TIP3P | AMBER | AMBER | F |
| 33 | Xie et al. (2007)[228] | SPC (flex) | ns | GROMACS | R |
| 34 | Banerjee et al. (2007)[60] | SPC | ns | ns | R |
| 35 | Longhurst and Quirke (2007)(6)[101−103] | SPC/E | REBO | MOLDSIM | F |
| 36 | Alexiadis and Kassinos (2008)[104,105,160] | various | AMBER | NAMD | R/F |

[a] R = rigid CNT, F = flexible CNT, n.s = not specified.

K. Disorder-to-order phase transitions to cubic water in (8,8) SWNTs at 298 K and to octagonal water in (10,10) at 248 K were found by Striolo et al.[139] Wang et al.[118] did not find any obvious ordered water structure inside *(n,n)* tubes with $n = 7, 8, 9, 10$, while Takaiwa et al.[148] found that, under the conditions investigated by Koga et al.,[145,149] the number of sides $n$ of the $n$-gonal configuration is higher in zigzag than armchair CNTs with approximately the same diameter.

A large number of articles have been devoted to this theme, but the results vary considerably with each other. It is still not clear, moreover, why different authors find different water structures at room conditions. This discrepancy may depend, as suggested by Wang et al.,[118] on the choice of the Lennard-Jones parameters used in the simulations or, as indicated by Guy et al.[150] while studying the structures of ice, on the appropriate treatment of the long-range forces by Ewald summation. Another hypothesis is that the way temperature and/or pressure is controlled in the MD simulation can play a certain role. Usually, thermostats and barostats add or remove a certain amount of energy from the system and the way this is done could have consequences on the water structure. In Figure 7, the values of $\epsilon_{C-O}$ and $\sigma_{C-O}$ used by some of the previous authors are gathered. The values are distinguished according to the structure observed in the CNT. Apparently, low values of $\epsilon_{C-O}$ and $\sigma_{C-O}$ seem to favor the formation of $n$-gonal structures, while at high values water molecules tend to present disordered structures. It must be noticed, however, that not all the results shown in Figure 7 were calculated at the same temperature and pressure. The simulations of Alexiadis and Kassinos[104] show that the water model plays a major role in determining the molecular structure of water in nanotubes. According to these results, the SPC/E model produces a perceptible pentagonal configuration while the structure coming from the TIP3P model is less clear. With a bit of imagination, it is possible to distinguish a pentagonal arrangement in this case too, but it is evident that the SPC/E structure looks more organized (see Figure 8). The TIP3P model, on the other hand, seems to favor a spiral-like layout of the water molecules in the nanotube.

Since none of these models was specifically designed for water in nanotubes, it is not possible to assess which of them works better until experiments will be able to "see" the details of the water structure in CNT. Up to now, experiments[113,114,151−153] only confirmed the existence of ordered water configurations inside nanotubes, but not their structure. These studies, moreover, highlight that water in CNTs undergoes structural transition from liquidlike (disordered) to solidlike (ordered) state between 200 and 250 K depending on the pressure and the CNT geometry. This fact deserves attention since a large majority of the MD simulations reported in Table 4 were calculated at temperatures that, accidentally, are close to the phase transition. MD involving phase transition is particularly sensitive to the choice of the simulation parameters and usually trickier than ordinary MD. Popular models like SPC, SPC/E, TIP3P, or TIP4P, for instance, produce poor agreement with water's melting point (giving melting points of 190, 215, 146, and 232 K respectively), while SPC, SPC/E, and TIP3P do not give ice Ih as a

**Table 5. General Overview of $H_2O$/CNT Simulations (Second Part)[a]**

| | (*n*,*m*) | *T* (K) | thermostat | *P* (bar) | barostat |
|---|---|---|---|---|---|
| 1 | (6−8,6−8)(10,10)(12,12) | 298 | ns | − | − |
| 2 | (6,6) | 300 | ns | 1 | n.s |
| 3 | (14−17,14−17) | 200−400 | NA | 500−5000 | ns |
| 4 | (5−10,5−10)(15,15) | 300 | L | 1 | L |
| 5 | (32,0)(64,0)(96,0) | 300 | B | − | − |
| 6 | (6,6) | 300 | ns | 1 | ns |
| 7 | (5−10,5−10)(12,12)(16,16) | 300 | NH | 1 | PR |
| 8 | (6,6) | 300 | ns | 1 | ns |
| 9 | (6,6) | 300 | ns | − | − |
| 10 | (6,6) | 298−598 | ns | − | − |
| 11 | (6,6) | 300 | ns | 1 | ns |
| 12 | (9−10,9−10) | 9−300 | ns | − | − |
| 13 | (5−10,5−10)(10,0)(12,0)(14,0)(16,0)(18,0) | 300 | B | − | − |
| 14 | (20,20)(30,30)(40,40) | 300 | B | − | − |
| 15 | (20,20)(30,30)(40,40) | 300−500 | B | − | − |
| 16 | (6,6)(10,10)(20,20)(10,0)(15,0)(13,7) | 298 | ns | − | − |
| 17 | (10,0)(8,4) | 298 | VR | − | − |
| 18 | (6,6) (8,8)(10,10)(12,12)(14,14)(16,16) | 300 | ns | 1 | ns |
| 19 | (12,0)(14,0)(17,0)(20,0)(24,0)(28,0) | 298−300 | ns | − | − |
| 20 | (5−10,5−10) | 300 | VR | − | − |
| 21 | (6,6) | 300 | B | − | − |
| 22 | (8,8)(10,10)(12,12)(20,20) | 298 | ns | − | − |
| 23 | (64,0)(72,0) | 300 | B | − | − |
| 24 | (5,5)(16,0) | 298 | NH | 1 | AH |
| 25 | (6−10,6−10)(12,12)(14,14)(16,16)(18,18)(20,20) | 300 | VR | − | − |
| 26 | (6,6)(10,10) | 275−370 | ns | − | − |
| 27 | (6,6)(10,0) | 300 | B | 1 | B |
| 28 | self-assembly of (5,5) into (10−25,10−25) | 300 | B | 1 | B |
| 29 | (10,10) | 100−337 | ns | − | − |
| 30 | (6−8,0)(8,1) | 300 | NA | 500−5000 | ns |
| 31 | (7−9,7−9)) | 300 | ns | − | − |
| 32 | (6,6) | 300 | ns | 1 | ns |
| 33 | (32,0) | 300 | ns | 1 | ns |
| 34 | (10,10) | 300 | G | − | − |
| 35 | (13−22,0) | 300 | B | 1−2000 | − |
| 36 | $d = 5.91-54.3$ Å (various chiralities) | 300 | L | 1 | NH |

[a] B = Berendsen, NA = Nosé−Andersén, L = Langevin, NH = Nosé−Hoover, PR = Parrinello−Rahman, VR = velocity rescaling, AH = Anderson−Hoover, G = Gaussian. Rows with the same cardinal number of Table 4 refers to the same simulations.

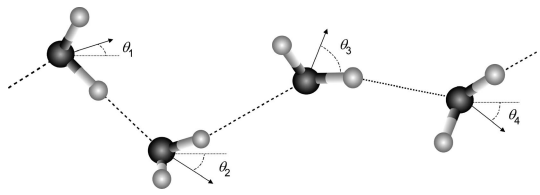


**Figure 4.** Schematic representation of water chain in small CNTs. (The angles $\theta_{1,2,3,4}$ represent the dipole orientation.)

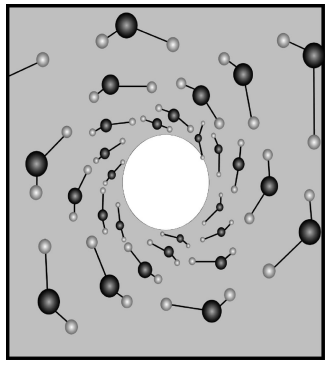

**Figure 5.** Schematic representation of helical structures in CNTs.

stable phase, replacing it with ice II or other unrealistic crystal structures.[154]

However, all the simulations, independently of the model used, show that water confined at the nanoscale presents

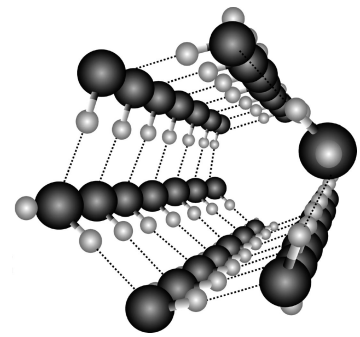

**Figure 6.** Schematic representation of hexagonal structure in CNTs.

certain characteristics that can considerably differ from those of bulk.[155] It displays, in particular, an intermediate state with both solid- and fluidlike properties. It has a solidlike symmetric structure, but at the same time, it shows a liquidlike degree of water−water hydrogen bonding (except for very small nanotubes). The possible existence of new phases of water inside CNTs can add a new prospective to the study of these systems. So far there have been many simulations under different conditions, but no systematic attempt to map the phase diagram of water in CNTs, which depends on *P* and *T* but also the diameter *d* of the nanotube. At the moment, however, this effort faces considerable difficulties due to the uncertainty in identifying the most appropriate water model in MD simulations and due to

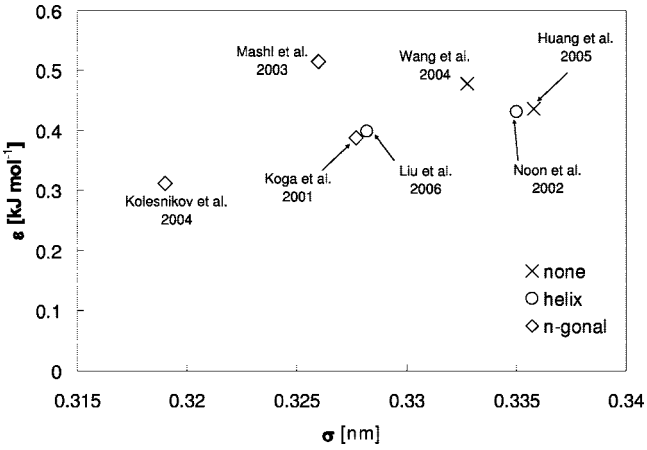


**Figure 7.** Water structures in the nanotube with respect to $\sigma_{CO}$ and $\epsilon_{CO}$.

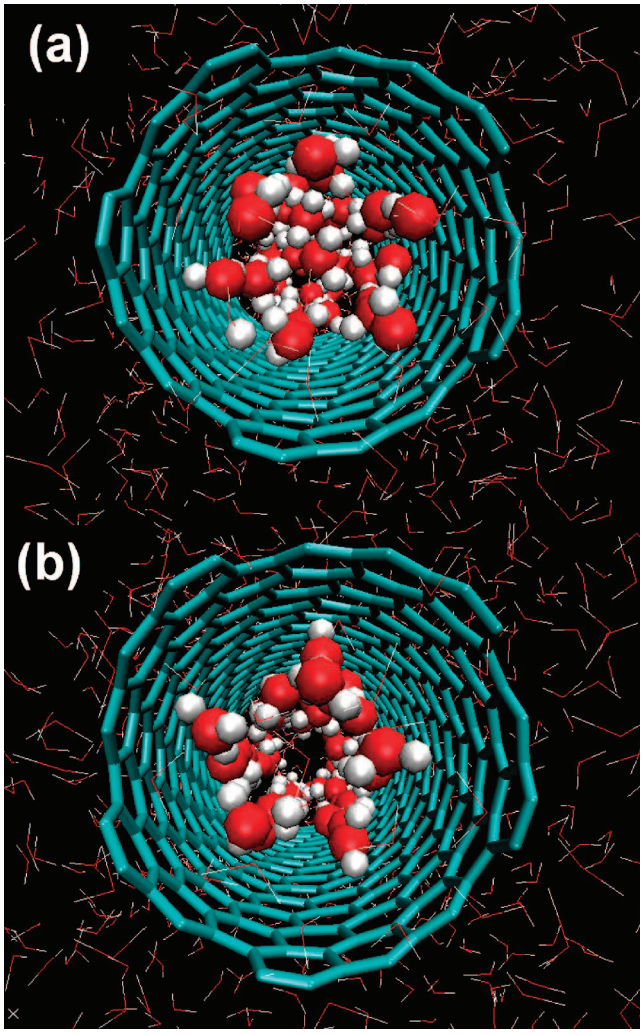


**Figure 8.** Atom distribution (snapshot) of water molecules in a (13,5) CNT calculated with the TIP3P (a) and SPC/E (b) water models.

technical problems connected with the microscopic size of the system in experiments.

## 7.2. Radial, Axial, and Total Water Density

The modification of its density is probably the most evident effect of the confinement of water within CNTs. The total density is strongly affected by the stratified structure described in the previous section. In Figure 9, the radial density profiles inside various nanotubes reported by different authors are compared. Figure 9 compares cases with different total densities; for this reason, dimensionless density (local density/total density) is used. In the (6,6) tube, there is sufficient space only for a single-molecular chain of water molecules. For this reason, only one peak is possible as Figure 9a shows. If the diameter increases, it is possible to have a second layer of water, which gives rise to a second peak. The number of layers $n$ that can be accommodated in a tube with radius $R_n$ depends on both $\sigma_{O-O}$ and $\sigma_{C-O}$ and can be calculated by the following equation:[118]

$$n = 1 + \frac{R_n - \sigma_{C-O}}{\sigma_{O-O}} \tag{17}$$

Above three or four layers, however, the water gradually loses memory of the wall and tends to assume again the bulk structure. Figure 9d compares the structure of water inside a (12,12) CNT, outside a (10,10) nanotube and on a flat graphite sheet and shows that, in all these cases, the bulk structure is practically restored after approximately 7−8 Å. The radial density profile, though, does not provide the complete picture, since the axial density is not constant.[98,99] In Figure 10, the axial density is showed according to Zhou et al.[99] for a (6,6), (8,8) and (9,9) CNT. The water distribution has a wavelike structure with a period that remains constant as the radius of the SWNT increases. The distance between two concentration peaks is approximately 2.5 Å, which is close to the distance of the centers of two consecutive hexagonal cells. Once the radial and axial densities are known, the total density should simply be the integral of these profiles in the nanotube. Things, however, are not so simple, since besides the radial and axial distribution, there is a third aspect of density that must be taken into account: the possible connection of the nanotubes with an external bath. There are, in fact, two kinds of simulations available in the literature: simulations where the total number of water molecules inside the nanotube is fixed to a certain value (typically 1 g/cm$^3$)[38,118,156−159] and simulations where the nanotube is in contact with an external bath and the molecules are free to enter and exit the nanotube.[98,99,104,105,160] The difference in the two cases consists not only of the number of molecules in the nanotube but also of the resulting pressure inside the CNT. There is, moreover, a third method, proposed by Hanasaki et al.[161−163] and called fluidized piston model (FPM), which does not take into account an external bath but adjusts the density in a certain section of the nanotube according to a certain procedure. In our discussion, this method is assimilated to the second category (water bath). The radial density profiles inside the nanotube are similar in the two cases as Figure 9 shows. Independently of their actual number in the CNT, therefore, the molecules always arrange themselves in an analogous stratified way (the structure within the layers, however, can differ). Figure 9 shows the radial profile inside the nanotube, but it does not say much on the geometrical structure ($n$-gonal, twisted etc.) of water in the CNT. The two snapshots of Figure 8, for instance, have two different molecular arrangements, but similar radial profiles. When the total number of water molecules is not fixed, the total density in the CNT is considerably lower than 1 g/cm$^3$. Alexiadis and Kassinos[105] report the complete profile of densities calculated with different water models and flexible/rigid nanotubes in the case of CNT + water bath (see Figure 11). This work

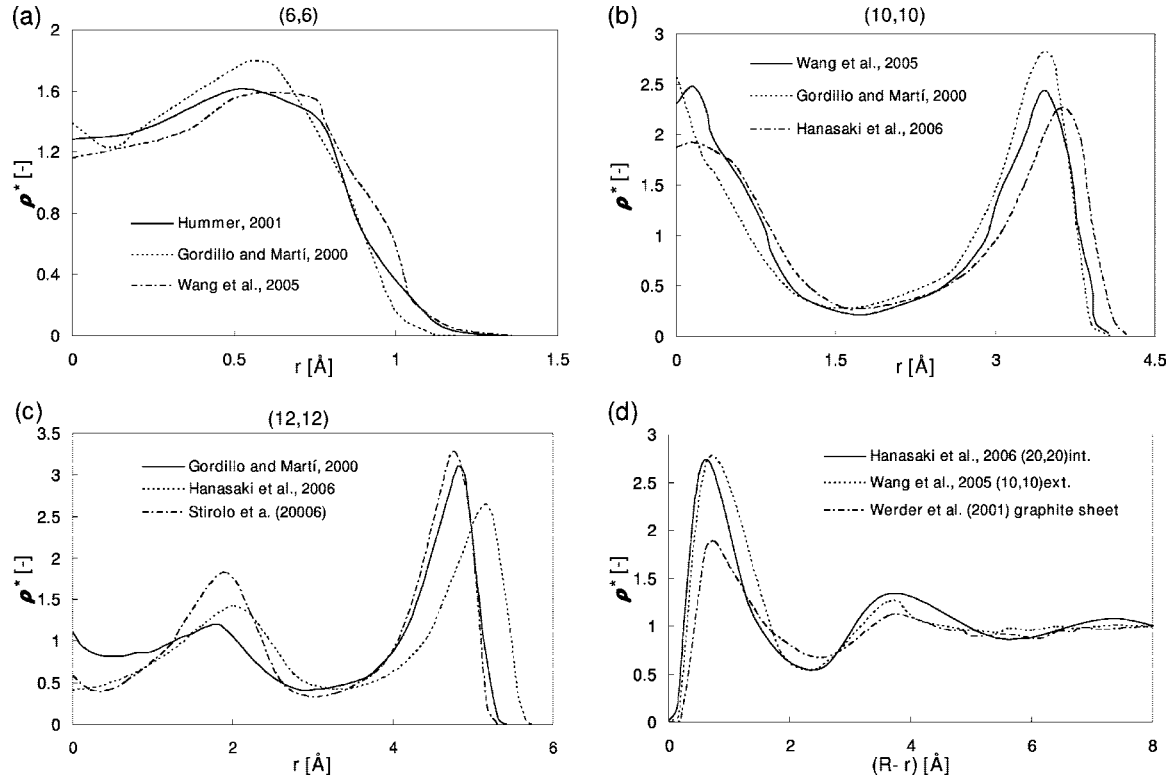


**Figure 9.** Dimensionless local water density ($\rho^* = \rho/\langle\rho\rangle$, where $\rho$ is the actual and $\langle\rho\rangle$ the total density) inside different nanotubes: (6,6) (a), (8,8) (b), (10,10) (c), and (12,12) (d), and outside a (10,10) nanotube (d). Note that, in (a, b, c) the abscissas represent the distance from the centner of the CNT, while in (d) the distance from the wall. The tube is open to a reservoir in Hummer et al. and Hanasaki et al. and closed in all the other cases. Adapted with permission from refs 38 (Copyright 2000 Elsevier), 98 (Copyright 2001 Macmillan Publishers Ltd.), 118 (Copyright 2004 Royal Society of Chemistry), 123 (Copyright 2001 American Chemical Society), 141 (Copyright 2006 American Institute of Physics), and 161 (Copyright 2006 American Institute of Physics).

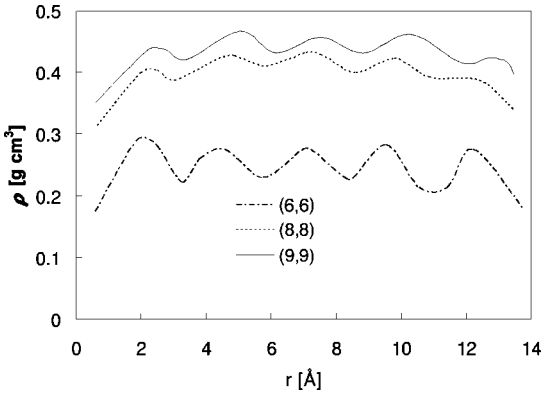


**Figure 10.** Axial water density inside (6,6), (8,8), and (9,9) nanotubes. The density is calculated on the basis of the total nanotube volume $(\pi/6)Ld^2$. Adapted with permission from ref 99. Copyright 2007 Institute of Physics.

provides a picture of how water molecules arrange themselves inside a CNT and produce a certain value of density according to the nanotube diameter. Water molecules, in fact, show at least two different ways of filling CNTs called "single-file mode" and "layered mode". The line labeled "single-file water" in Figure 11 indicates the narrowest nanotubes, which can contain only a single file of water molecules. In this case, if the size of the CNT is reduced, for instance, from (6,6) to (8,2), the number of molecules per nanotube length does not change very much (see Figure 12). The volume of the nanotube, however, decreases more significantly and, consequently, the density augments as shown in Figure 11. If the diameter increases and more than one water layer is allowed into the nanotube, the behavior changes dramatically. In fact, when the diameter is in the "layered mode" (region indicated with "waters layers" in Figure 11) the arrangement of water molecules near the walls assumes the typical layered structure,[38] which has a higher void fraction and, consequently, lower density. If we augment the diameter further, the distance between the walls and the core of the nanotube increases and the water molecules located at the center of the CNT behave like in bulk ("bulk mode" in Figure 11).

The following correlation was suggested in order to approximate the value of the density in nanotubes of different diameters in the layered mode.[160]

$$\begin{cases} \dfrac{\rho}{\rho_0} = 1 - \dfrac{\rho_1^*}{(d/d_1^* + 1)^2}, \quad \text{with } d_1^* = 20.6 \text{ Å}, \\ \qquad\qquad \rho_1^* = 1.4 \text{ g/cm}^3 \text{ for } d < 24.8 \text{ Å} \\ \dfrac{\rho}{\rho_0} = 1 - \dfrac{\rho_2^*}{(d/d_2^* + 1)^2}, \quad \text{with } d_2^* = 55.0 \text{ Å}, \\ \qquad\qquad \rho_2^* = 0.6 \text{ g/cm}^3 \text{ for } d \geq 24.8 \text{ Å} \end{cases} \tag{18}$$

The value $d = 24.8$ Å divides the "layered" from the "bulk" mode, where water molecules arrange themselves like in bulk conditions.

## 7.3. Hydrogen Bonds

Many thermodynamical properties (e.g., melting and boiling point) of water depend on the strength of the hydrogen bonds (H-bond) formed among $H_2O$ molecules.

The H-bond is a special type of attractive interaction that exists between an electronegative atom and a hydrogen atom bonded to another electronegative atom. Since water has two hydrogen atoms and one oxygen atom, two molecules of water can form a H-bond between the O and the H atoms. Each water molecule can form up to four hydrogen bonds at the same time (two through its two lone pairs, and two through its two hydrogen atoms). The average number of H-bonds per molecule calculated in bulk water varies approximately from 2.3 to 3.8[164,165] according to the water model and the way used to define the H-bond. In MD simulations of water in CNT, the geometrical definition[166] of H-bond is the most used. According to this definition, a H-bond must satisfy the following three conditions.

1. The distance between the oxygens of both molecules has to be smaller than a certain threshold value $R_{OO}$.

2. The distance between the oxygen of the acceptor molecule and the hydrogen of the donor has to be lower than a certain threshold value $R_{OH}$.

3. The bond angle between the O−O direction and the molecular O−H direction of the donor, where H is the hydrogen which forms the bond, has to be lower than a certain threshold value $\phi$.

The values of $R_{OO}$, $R_{HO}$, and $\phi$ can vary from work to work.[38,105,118,146] A common result of all the articles taken into account is that the average H-bond of water molecules decreases in confined space. The smaller the tube, the lower the number of H-bonds. This value reaches approximately 1−1.5 bonds for small CNTs, where only a monomolecular layer of water is allowed. This behavior is easily understood considering that in confined space $H_2O$ molecules have a lower coordination number; the extreme case of Figure 12 gives a clear picture of this concept. In Figure 13, information on the average number of H-bonds (calculated according to $R_{OO}$ = 3.3 Å, $R_{HO}$ = 2.4 Å and $\phi$ = 30°) as a function of the nanotube diameter calculated with different water models and rigid/flexible nanotubes is gathered.[105] The labels "single-file water", "water layers", and "bulk model" were kept in Figure 13 for comparison with density (Figure 11) and self-diffusion (see next section), although in the present circumstance the separation between these two zones is not as clear as in the other cases.

The modification of the number of H-bonds is not the only consequence of confinement. The probability distribution of the H-bonds, in fact, also changes and becomes more concentrated toward the high energies as reported by Hummer et al.[98] (Figure 14). The confinement sharpens the hydrogen-bond energy distribution, shifting the mean toward higher values, but resulting in a lower population in the high-energy tail. This resulting modification on the hydrogen-bonding net has strong consequences on many properties of water, as is explained in the next sections.

## 7.4. Filling Carbon Nanotubes with Water

The filling of small CNTs like (6,6) or (5,5) by water molecules is not a simple phenomenon and, at first glance, it appears impossible. As was shown in the previous sections, a water molecule loses a certain number of hydrogen bonds when it enters CNTs and the van der Waals attraction of the hydrophobic nanotube cannot compensate the loss. This means that if we limit our analysis to this consideration, water molecules would have no reason to move inside a small CNT and the phenomenon would appear impossible. However, both MD and experiments show that water can fill even small

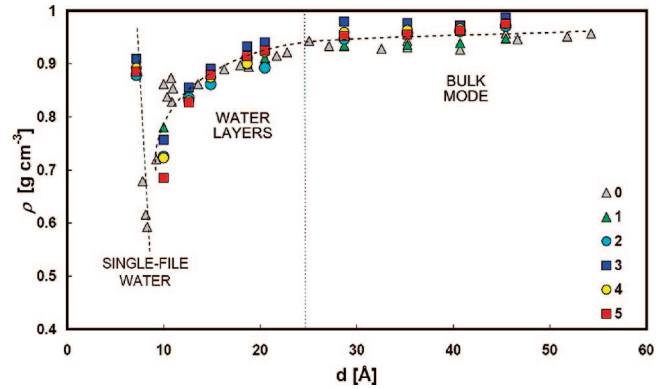


**Figure 11.** Bulk density versus diameter. The data are divided into six different groups: (0) TIP3P water model/rigid CNT, (1) TIP3P water model/flexible CNT, (2) SPC/E water model/rigid CNT, (3) flexible TIP3P water model/rigid CNT, (4) flexible SPC water model/rigid CNT, and (5) flexible SPC water model/flexible CNT. In this case, the density is calculated on the basis of the empty nanotube volume, which is not $(\pi/6)Ld^2$, but $(\pi/6)L(d - \sigma_{CO})^2$ in order to take into account the occupancy of carbon atoms.

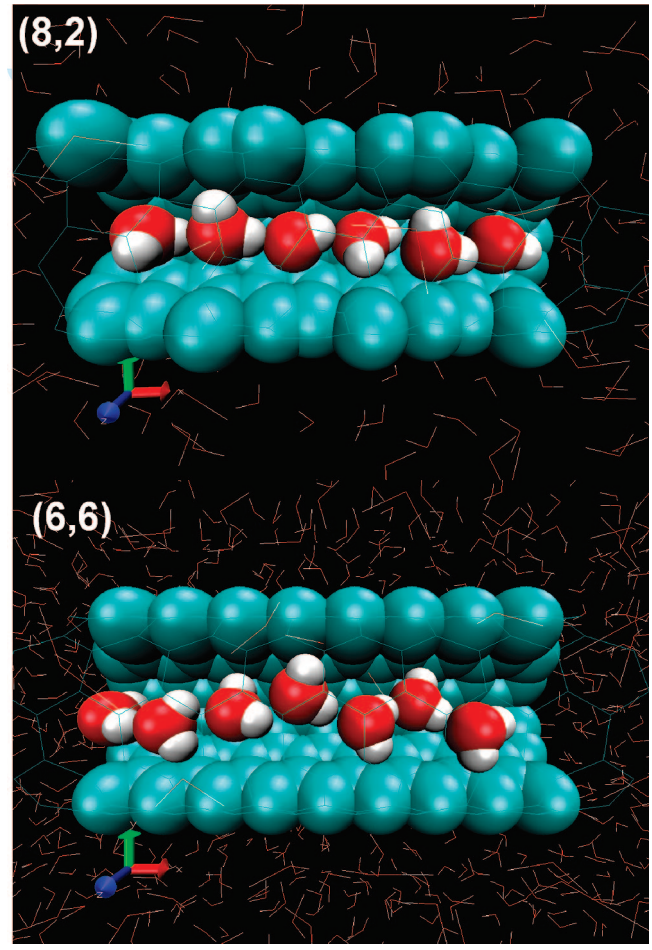


**Figure 12.** Single-file distribution of water molecules in (8,2) and (6,6) carbon nanotubes (part of the tube was removed for visualization purposes).

(5,5) nanotubes, where it loses more than half of its H-bonds. The explanation for this behavior depends on the fact that the entrance of the first water molecules is thermodynamically disadvantaged, but the filling of the whole nanotube is favorable. Wage et al.[167] reported the free energy of the process of penetration of water molecules inside a 27 Å long (6,6) nanotube (Figure 15). The free energy increases until a certain point and then, when the nanotube is completely

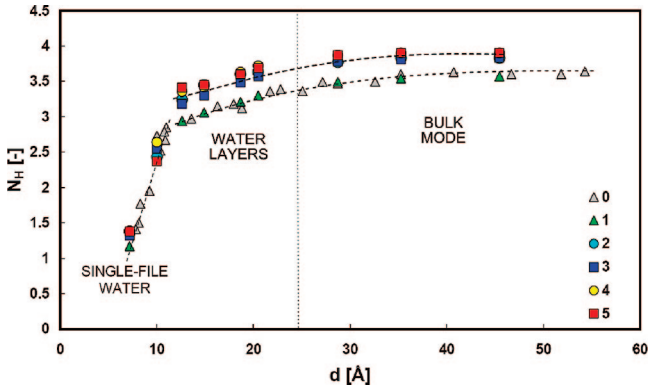


**Figure 13.** Hydrogen bonding (calculated with $R_{OO} = 3.3$ Å, $R_{HO} = 2.4$ Å, and $\phi = 30°$) versus diameter. The data are divided into six different groups: (0) TIP3P water model/rigid CNT, (1) TIP3P water model/flexible CNT, (2) SPC/E water model/rigid CNT, (3) flexible TIP3P water model/rigid CNT, (4) flexible SPC water model/rigid CNT, and (5) flexible SPC water model/flexible CNT.

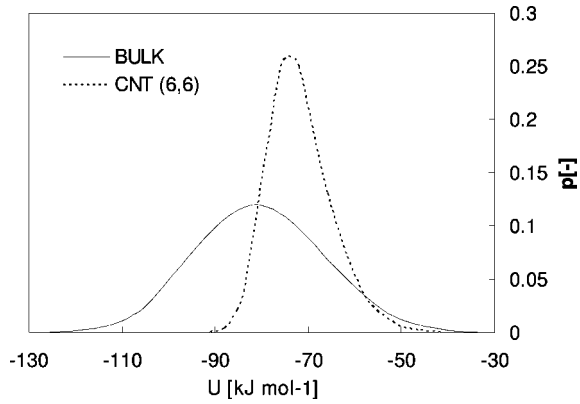


**Figure 14.** Probability distribution of the water binding energies (H-bonds) inside a (6,6) CNT and in the bulk. Adapted by permission from Macmillan Publishers Ltd.: *Nature* (ref 98), copyright 2001.

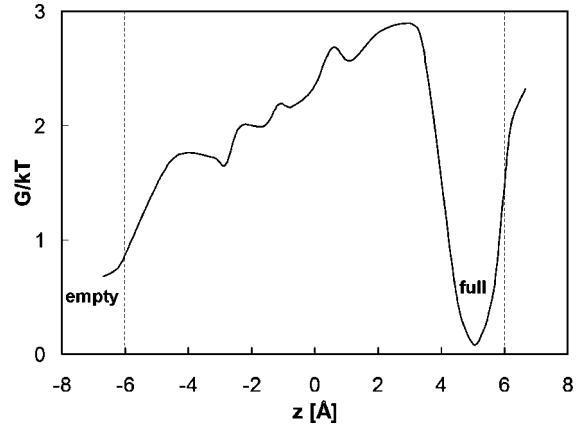


**Figure 15.** Free energy versus water penetration inside a (6,6) nanotube 12 Å long. Adapted with permission from ref 167. Copyright 2002. American Institute of Physics.

filled, it drops suddenly. Furthermore, the first part of the curve, where the free energy increases, shows a kind of staircase behavior, whose steps correspond to the entrance of an additional water molecule. Once the first water molecule is in the nanotube, the penetration of an additional molecule is less costly in terms of free energy. The system, therefore, can, molecule after molecule, fill completely the nanotube and reach the free energy minimum. The two states

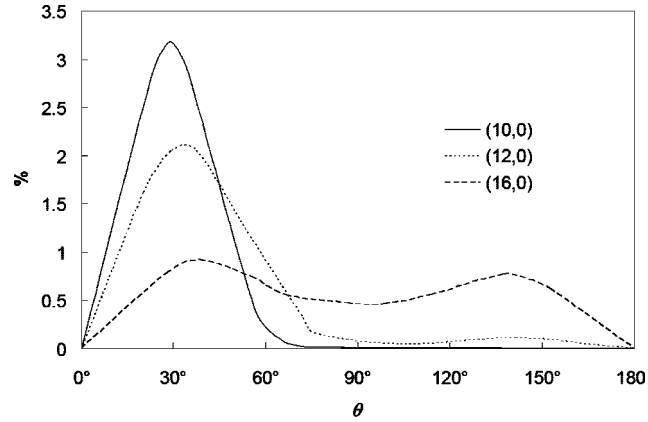


**Figure 16.** Percentage of water molecule in (10,0), (12,0), and (16,0) CNTs forming an angle $\theta$ (see Figure 4) between the nanotube axis and the dipole moment. Adapted by permission of the PCCP Owner Societies, from ref 118 (DOI: 10.1039/b313307a). Copyright 2004 Royal Society of Chemistry.

with lower energy (completely empty and completely full) have approximately the same energy justifying the observed pulselike behavior.[98,167] There are, however, two additional remarks that must be taken into account. First, these results are very sensitive to the C−O interaction and slightly modified $\sigma_{C-O}$ and $\epsilon_{C-O}$ parameters can lead to completely different results.[98,167] Second, these simulations were carried out for relatively short nanotubes and there is not investigation for longer CNTs.

## 7.5. Dipole Moment

The nonuniform distributions of positive and negative charges in water molecules lead to a dipole moment, which points toward the positive hydrogen atoms, of approximately 1.85 D (debye) for isolated water molecules (or gas phase) and of approximately 2.95 D for bulk liquid water. The orientation distribution of water molecules within CNTs is usually given by the angle $\theta$ between the dipole moment and the positive direction of the $z$-axis (see $\theta_{1,2,3,4}$ in Figure 4) and depends on the combination of van der Waals and electrostatic forces. Hydrogen atoms, for instance, tend to be located closer to the carbons since $\sigma_{C-O} > \sigma_{C-H}$.[38,146] Electrostatic forces, on the other hand, tend to drive as far as possible charges with the same sign. Therefore, the result is that $H_2O$ molecules located near the walls are likely to have one of the O−H bonds, which points toward the CNT, while the other tends to align itself with the nanotube axis.[98,167] Figure 16 shows the orientation of water dipole inside (10,0), (12,0), and (16,0) CNTs. Apparently, the chirality does not particularly affect these profiles, which depend mainly on the value of the diameter. In general, the distribution of $\theta$ is more narrow in small nanotubes than in large ones. In fact, by increasing the CNT diameter, any $\theta$ value between 0° and 180° becomes possible. This fact may be explained, according to Wang et al.,[118] by two factors. One is that water molecules tend to become more disordered in wider CNTs. The other is that the flipping of the dipole becomes more frequent inside wider CNTs. The flipping of the dipole orientation, however, is a controversial issue. According to certain authors[98,167] water molecules flip frequently orientation within the CNT (every 2−3 ns in average). This means that the (10,10) profiles reported in Figure 16, for instance, would have a second symmetric peak at ∼150° (see, for instance, the nonpolar curve in Figure

20). Not everybody, however, agrees with this conclusion. Zhou et al.[99] found that the molecules flip continuously in the (7,7) (every 0.5−0.7 ns in average), often in the (8,8) (every 1−2 ns in average), but they do not flip in the (9,9). Wang et al.[118] reported profiles similar to those shown in Figure 16, which denote absence of flipping. Mann and Halls[110] studied a (6,6) CNT with ab initio molecular dynamics techniques showing that dipolar flipping is a rare event under ambient conditions but, since this phenomenon has a characteristic time scale of nanoseconds, it can hardly be seen in ab initio simulations that usually cannot be run for more than a few picoseconds.

Besides the orientation, the strength of the dipole plays an important role on certain water properties like the surface tension. The value of the dipole moment, however, cannot be calculated with classical methods. Each water model has its own dipole moment determined by the parameters of the model (optimized for bulk conditions) and cannot change during the simulation. In order to calculate the dipole moment, the information about the electronic structure of the atoms is required and quantum methods are necessary. Mann and Halls[110] used first-principles molecular dynamics to calculate the electric dipole moment of water inside a (6,6) nanotube. They found an average dipole moment per water molecule of 0.75 D, which is lower than that of both isolated (1.85 D) and bulk water (2.95 D). They repeated the same calculation on the water file with the CNT removed and they found a dipole moment of 2.7 D. This means that the interaction between the water molecules and the nanotube plays a key role on the dipole moment and, in particular, it reduces the dipole moment of CNT + water systems. There is not, however, a general agreement on this point. Dellago and Naor,[168] for instance, reported a dipole moment of 2.7 D from DFT calculations of water in (6,6) nanotubes.

## 7.6. Proton Transport in Water

When an excess proton is placed in water, it will attach itself to a water molecule, forming a hydronium cation.[169] There are two solvation structures of hydronium in water: the "Eigen" cation $H_3O^+$ and a second solvation complex, in which the excess proton cannot be assigned to a particular oxygen, but rather appears to be located directly between two water molecules. The latter is the $H_5O_2^+$ "Zundel" cation, which plays a major role in the proton transfer process in bulk phase (there are many intermediate solvation structures of protons in bulk water; the Eigen and Zundel cations must be seen as the two extreme cases). In confined water, where the $H_2O$ molecules are particularly well aligned, proton transport can be particularly fast due to the so-called Grotthus mechanism.[170] In this case, the proton hops in a concerted fashion across the whole array of water molecules as exemplified on the left part of Figure 17. The phenomenon was observed in (6,6) CNTs by Mann and Halls[110] through ab initio methods. Dellago et al.,[109] on the other hand, showed that the transfer mechanism can be limited by hydrogen-bonding defects in the water-wire. These defects are called L-defects and D-defects (Figure 17) and can represent an effective barrier for rapid proton conduction. Lately, this topic has received a certain attention because narrow CNTs can be used as prototype for studying more complicated biological structures like aquaporins,[171] which, discovered for the first time in 1992, are transmembrane channel proteins found in cell membranes of all life forms. The effect of charged[172] or polarized[173] CNTs was studied

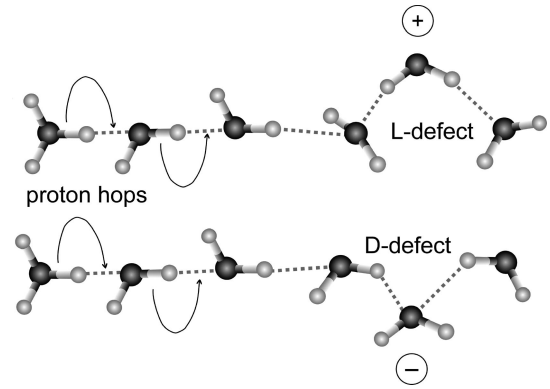


**Figure 17.** The Grotthus mechanism of proton hops among water molecules on the left. On the right, the effect of positive or negative partial charges, which creates respectively L- and D-defects in the water chain. Once the proton meets a L- or D-defect, it cannot propagate further.

in order to investigate how electrostatic forces can affect proton transport in nanochannels. The results show that, in the proximity of local charges, hydrogen-bonding defects can arise. If the charge is positive, electronegative oxygens are attracted by the walls and L-defects are formed. If, on the other hand, the charge is negative, the hydrogens are attracted by the walls and D-defects arise (Figure 17). In Figure 20, water dipole orientations in (6,6) polar and nonpolar CNTs are compared. The presence of the electric field causes an orientational change within the chain of water molecules. The peaks of the nonpolar distribution (30° and 150°) are shifted to 25° and 155°. Additionally, there is a peak at 90°, which indicates the presence of an L-defect. These observations helped to improve the current understanding of the behavior of biological channels like aquaporins and, in particular, the mechanism used to impede proton conduction inside living cells.[174]

## 7.7. Transport Properties

Berezhkovskii et al.[175] and Kalra et al.[22] show that water transport in nanoscale pipes or tubes is stochastic in nature, dominated by thermal fluctuations, and, in small nanotubes, can be described well by a one-dimensional continuous time random walk model. Water transport in CNT is a fast phenomenon and it appears frictionless due to the smooth interior walls of the CNT. These conclusions were supported by subsequent experiments on membranes of CNTs.[176]

Specific transport properties of water in CNTs can be calculated from molecular dynamic simulations. Liu and Wang[157] calculate self-diffusivity ($D$), thermal conductibility ($\lambda$) and shear viscosity ($\eta$) by means of the Einstein[177] and Green−Kubo[178] equations

$$D = \lim_{t\to\infty} \frac{1}{2kt}\langle |r(t) - r(0)|^2 \rangle \tag{19}$$

$$\lambda = \frac{1}{k_B T^2 V}\int_0^\infty \langle S(t)S(0)\rangle \, dt \tag{20}$$

$$\eta = \frac{1}{k_B T V}\int_0^\infty \langle J_v(t)J_v(0)\rangle \, dt \tag{21}$$

where $r(t)$ is the position of the center of mass of water molecules at time $t$, $k$ the dimensions of the system, $k_B$ the Boltzmann constant, $T$ the temperature, $V$ the volume of the simulation box, $S$ the heat flux, and $J_v$ the momentum flux.

Water in carbon nanotubes shows anisotropic properties due to the fact that $H_2O$ molecules have higher collision frequency in the axial direction. In the radial direction, $H_2O$ presents a stratified structure, which tends to isolate each layer of water from the others and, consequently, to reduce molecular collision in this direction. This explains why all the transport properties radially are lower than in the axial direction. According to Liu and Wang,[157] however, the diffusivity in SWNTs is lower (1 order of magnitude in small nanotubes) than that of the bulk, and it decreases as the diameter decreases. These results, nevertheless, disagree with those of other research groups,[22,105,175,176] who found fast transport in nanotubes. This disagreement depends on the fact that Liu and Wang calculated the self-diffusivity at fixed densities (from 0.875 to 1.25 g $cm^{-3}$), which are much higher than the spontaneous density (we define "spontaneous" or "natural" the density obtained leaving the water molecules to spontaneously enter the nanotube from an external bath) of water molecules in CNT (see section 7.2). As a consequence, the mobility of the molecules in the crowed nanotube is reduced.

Another point that must be stressed is that eq 19 assumes Fickian diffusivity, but this is not the only possible mechanism of diffusion. Striolo[140] studied water diffusion in infinitely long narrow carbon nanotubes, taking into account non-Fickian behaviors (that is, the molecular mean-square displacement does not scale with $t$). These departures from the Fick law are caused by the fact that water molecules confined in a narrow one-dimensional channel are prevented from passing each other. Previous studies,[179,180] in fact, suggested that in small nanotubes, molecules should exhibit a kind of subdiffusive behavior, known as single-file diffusion, where the mean-square displacement (MSD) scales with $t^{1/2}$ instead of $t$ (this behavior is expected to occur only in infinitely long, or toroidally closed, tubes and not in open tubes in contact with a reservoir). The diffusion of oxygen molecules inside (10,0) CNTs,[181] for instance, follows this mechanism with MSD $\propto t^{\alpha}$ where the exponent $\alpha$, under certain conditions, is less than unity. There is, however, a third possibility, which happens when confined molecules move in a highly coordinated fashion. This is called ballistic transport and the MSD scales with the square of time. Ballistic transport is observed when the mean free path of the particle is bigger than the size of the box that delimits the medium through which the particle travels. In this circumstance, the particle alters its motion mostly by hitting against the walls rather than colliding against other particles. It is called ballistic since it can be described by Newtonian dynamics instead of Langevin dynamics, which is more indicated in the case of Brownian motion.[182]

The three motion mechanisms can be mathematically described as

$$D \propto \begin{cases} \dfrac{|r(t+\Delta t)-r(t)|^2}{\Delta t}, & \text{Fickian diffusion} \\ \dfrac{|r(t+\Delta t)-r(t)|^2}{\Delta t^{1/2}}, & \text{single-file diffusion} \\ \dfrac{|r(t+\Delta t)-r(t)|^2}{\Delta t^{2}}, & \text{ballistic transport} \end{cases} \tag{22}$$

MD simulations of the diffusion of water molecules inside (8,8)[140] and (6,6)[183] nanotubes show that water molecules initially undergo ballistic transport, which, in the long run, changes into Fickian. This seems to indicate that water has the same macroscopic diffusion mode both in bulk and in confined space. According to Mukherjee et al.,[183] this depends on the fact that water molecules present a strong correlation due to hydrogen bonding. Therefore, they are highly coordinated like in ballistic mode ($|r(t+\Delta t)-r(t)|^2 \propto \Delta t^2$) but, at the same time, they move in a monodimensional configuration like in single-file diffusion ($|r(t+\Delta t)-r(t)|^2 \propto \Delta t^{1/2}$). The compromise between these two opposite situations results in the apparent Fickian diffusivity ($|r(t+\Delta t)-r(t)|^2 \propto \Delta t$) observed. Thus, the exponent of $\Delta t$ in eq 22 is very close to 1 in both bulk and confined water, but this is just a coincidence since the mechanisms of diffusion are very different in the two cases.

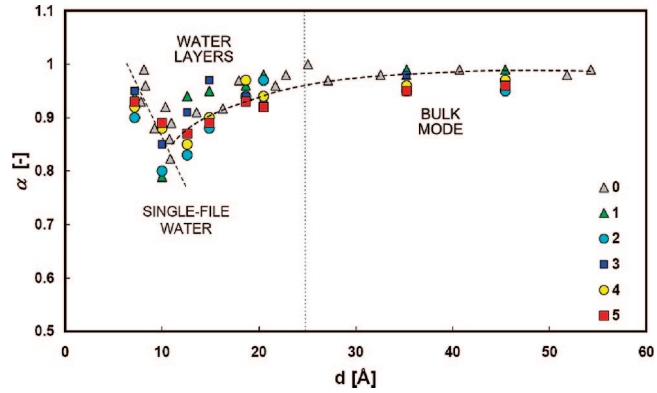


**Figure 18.** Self-diffusivity parameter α versus nanotube diameter. The data are divided into six different groups: (0) TIP3P water model/rigid CNT, (1) TIP3P water model/flexible CNT, (2) SPC/E water model/rigid CNT, (3) flexible TIP3P water model/rigid CNT, (4) flexible SPC water model/rigid CNT, and (5) flexible SPC water model/flexible CNT.

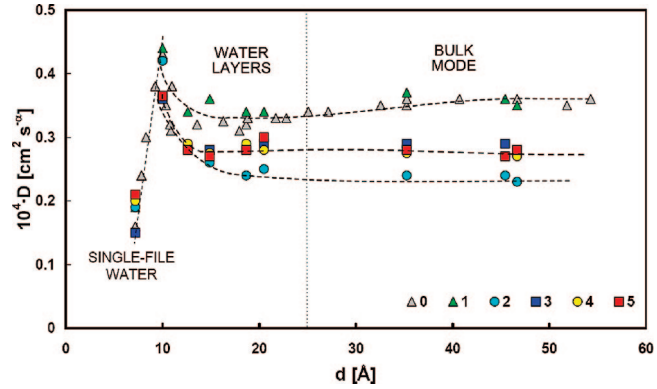


**Figure 19.** Self-diffusivity coefficient $D$ versus nanotube diameter. The data are divided into six different groups: (0) TIP3P water model/rigid CNT, (1) TIP3P water model/flexible CNT, (2) SPC/E water model/rigid CNT, (3) flexible TIP3P water model/rigid CNT, (4) flexible SPC water model/rigid CNT, and (5) flexible SPC water model/flexible CNT.

Self-diffusivity of water in nanotubes of different size using "natural" density is investigated in Alexiadis and Kassinos.[105] The calculated values of α and $D$ ($|r(t+\Delta t)-r(t)|^2 \propto \Delta t^{\alpha}$ in eq 22) are shown in Figures 18 and 19. In the case of self-diffusion $D$, Figure 19 shows that different models yield different values of $D$. This fact, however, is consistent with results of bulk water diffusivity coming from comparisons among different water models.[184,185] Figure 19 compares quantities with different units since the value of α is variable and, therefore, the figure has only qualitative value. Both Figures 18 and 19 exhibit the discontinuous profile already observed in Figure 11. In the single-file mode,

the diffusion exponent $\alpha$ increases when the diameter decreases, while in the layered mode the opposite happens. This phenomenon has the same explanation already discussed in Striolo et al.[140] and Mukherjee et al.[183] In small nanotubes, the molecules form a molecular wire, which should give single-file diffusion. Water molecules, however, form hydrogen bonds, which can enhance coordination and, consequently, the value of $\alpha$. It is true that, according to Figure 13, the number of H-bonds decreases at low diameters, but in this case, the hydrogen bonds are mostly oriented toward the axis of the nanotube. In the bulk, the H-bonds are almost 4, but water molecules are pulled or pushed isotropically by their H-bonds without any preferential direction. In small nanotubes, the number of H-bonds is between 1 and 2, but on the other hand, they act mainly on the axis of the nanotube favoring coordination, hence $\alpha$, in this direction. We see here another example of how the modification of the hydrogen-bonds net can affect the properties of water inside nanotubes.

## 8. Driven Flow

The effect of driving forces on $H_2O$ flow was investigated in a number of simulations. The case of osmotically driven flows in membrane systems made of nanotubes, for instance, is a classical example of a practical application requiring the calculation of driven flow. Another, more theoretical, interest on this subject focuses on the gradual loss of the validity of the continuum hypothesis at high Knudsen numbers. At the macroscopic scale, the steady-state flow within a tube is described by the well-known Poseuille equation. By decreasing the size of the tube to the nanoscale ($d = 1-20$ Å) this equation gradually loses its validity, but in the case of simple Lennard-Jones fluids[131] the typical Poseuille parabolic profile is not completely lost and it can be used as a first approximation if a slip velocity is taken into account at the walls.

The most widely used methods to impose a driving force on the flow are called "gravity fed"[131,186] and "dual control volume grand canonical molecular dynamics" (DCV-GCMD).[187] In the case of gravity-fed flow, an external gravitational-like field is uniformly applied to the system and the particles are driven by this field. Initially, the magnitude of the applied field was decided after some trial and error for each specific situation. More recently, an adaptive force algorithm has been proposed[188,189] to directly assign the streaming velocity from the beginning. In all cases, the applied gravitational field is unrealistically high ($\sim 10^9$ m $s^{-2}$), but the method has the advantage of low computational costs. The main problem with this approach, however, is that the uniform field is not particularly suitable for studying properties of systems which are essentially inhomogeneous in the flow direction.[163] In addition, it is not certain that the collective behavior of polyatomic or complex molecules under a strong gravitational field is always the same as those under an actual pressure gradient.

The DCV-GCMD method[138] drives the particle flow with a chemical potential (or pressure) gradient. It is a hybrid algorithm of MD and the grand canonical Monte Carlo (GCMC) method, and it is used mainly for diffusive flow through microscopic pores. After each time step, a certain number of GCMC steps are conducted to insert or delete particles in the system. The disadvantage of this method lies in the high computational costs, especially in the case of dense fluid systems or polyatomic molecular systems.

Additionally, some other approaches drive the fluid flow by means of a pressure gradient.[190,191] These methods, however, have never been used for nanotubes and, at the moment, it is not possible to assess their advantages and disadvantages in the case under study.

A new approach, called fluidized piston model (FPM), was recently proposed by Hanasaki et al.[163] An external gravity-like field is imposed only to the fluid located in a first section of the nanotube. The molecules in this section act as a fluidized piston that presses the rest of the fluid. The central part of the CNT is used for analysis, while the inlet and outlet are needed only for numerical reasons. Periodic boundary conditions cannot be used with this approach since the authors found that unrealistic interactions can arise if inlet and outlet are connected. This method seems to have certain advantages over the gravity-fed flow approach, but further investigation and comparison with other methods is required.

All these methods try to impose "by force" the driven flow and, as consequence, they pay a price in terms of unrealistic gravitational-like field or other drawbacks. If the goal is the study of osmotically driven CNTs membranes, there is an alternative to the previous approaches, which involves the simulation of nanotubes in a water/solute environment. In Kalra et al.,[22] for instance, the osmotic pressure is not imposed but it appears naturally as a consequence of the solute. This method gives a more physical description of the system, but, on the other hand, besides the $H_2O$ molecules within the CNT, an external bath with the solute molecules must be also taken into account.

## 9. Charged Carbon Nanotubes

The electric field produces significant effects on the nanofluid properties, such as the density distribution, the polar orientation, the filling rate, and the transport behavior and, at least theoretically, it is possible to control the fluid velocity of water by changing the charge on the SWNT. Huang et al.[192] added electric charges to a (10,10) SWNT. Their MD simulations show that, in a negatively charged nanotube, regular water structures, such as the ones described by Koga et al.,[145] are more likely to appear. In this case, moreover, the water molecules are highly polarized with all the hydrogen atoms pointing to the walls. On the contrary, when the charge is positive, oxygen atoms are attracted and hydrogen atoms are repelled, resulting in polar orientation of water opposite to that seen in the previous case.

Charge affects not only the structure of the water but also its dynamics.[60,192] An uncharged CNT is hydrophobic and water molecules enter into neutral nanotubes as previously indicated (section 7.4). When the CNT is charged, depending on the sign of the charge, either hydrogens or oxygens are attracted by the carbons and, as confirmed by experiments,[193] the nanotube becomes hydrophilic. In this case, water molecules can fill SWNTs much faster. A $-0.115e$ (10,10) charged CNT, for instance, is completely filled in a few picoseconds, while the same neutral nanotube requires approximately 50 ps.[192] The water−wall interactions facilitate the filling of the CNT, but, on the other hand, they hamper the flow of water through the nanotube. Charged nanotubes are, therefore, more indicated for containing water, while neutral ones for conveying it.

Opportunely designed charge patterns, on the other hand, can confer to the nanotube characteristics, which differ from those of uniformly charged CNTs. In particular, this circumstance can find applications in the study of membranes

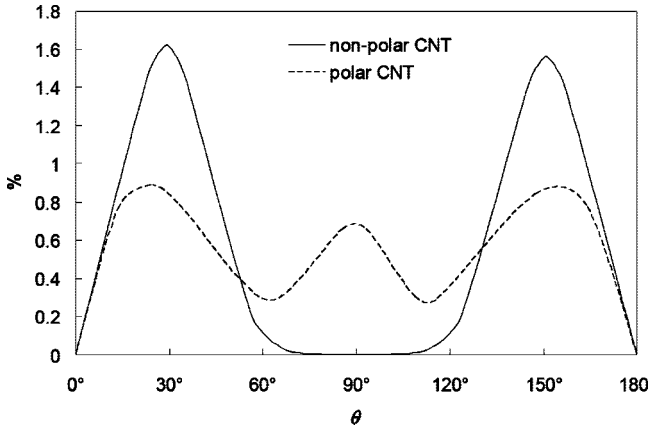


**Figure 20.** Percentage of water molecule in (6,6) polar and nonpolar CNTs forming an angle $\theta$ (see Figure 4) between the nanotube axis and the dipole moment. The central peak in the polar profile denotes an L- or D-defect. Adapted with permission from ref 173. Copyright 2005 American Chemical Society.

for desalination. In fact, Banerjee et al.[60] showed that alternate rings or axial bands of positive and negative charges on SWNTs reduce considerably ion intake and increase, as a consequence, the performance of water-purifying devices based on such CNTs.

## 10. Polarizable Carbon Nanotubes

A certain number of ab initio studies[194−197] demonstrated the polarizability of carbon nanotubes due to the delocalized $\pi$-electrons. Walther et al.[115] took into account the electrostatic interactions between water molecules and point quadrupole moments on the carbon atoms but, the contribution of these terms was found to be negligible. Later, Arab et al.[198] showed that the electric field created by a single $H_2O$ molecule located in a CNT can significantly polarize the nanotubes. In turn, the resulting electric field created by the polarized nanotube can interact with the water dipole resulting in total contribution to the global energy of approximately 45%. The potential energy profiles of a single TIP3P water molecule at various positions inside a (6,6) CNT were studied by Lu et al.[199] They found that the major contribution to the total potential energy, in general, comes from the van der Waals forces, but at the edges of the CNT, the shape is dominated by the electrostatic interaction between the water point charges and the charges induced on the nanotube. The existence of edge dipoles creates bumps in the total energy, which may slow the transport of water molecules through SWNTs (Figure 21). Moulin et al.[200] carried out the first MD simulation in order to quantify the polarization of a carbon nanotube in contact with more than one water molecules at room temperature. The results coming from their simulations show that, if an empty nanotube is immersed in water, the polarization effects are basically negligible and the liquid water around the nanotube is a quasi-nonpolar environment. Larger polarization effects are obtained considering water inside the nanotube, but also in this case the polarization contribution to the total energy per molecule reaches at most 8%. Dumitrica et al.[195] found a significant static dipole moment, due to the curvature, in empty CNTs. The effect of the (6,6) CNTs curvature-induced dipole moment on water flow has been studied by Zimmerli et al.,[173] who found that polarization has consequences similar to those seen in the case of static charges (section 9). The CNT, in fact, becomes more hydrophilic and tends

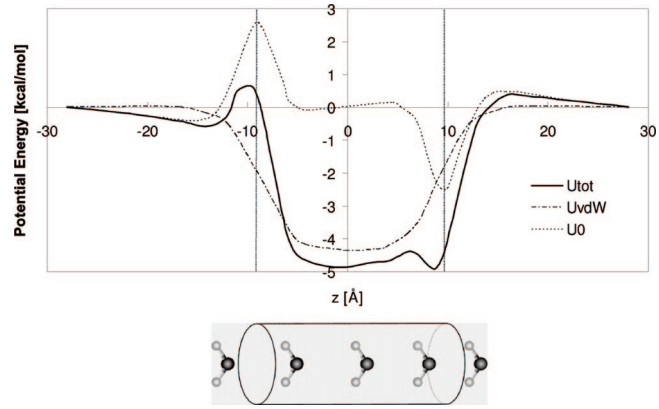


**Figure 21.** Potential energy of a water molecule inside a polarizable CNT according to Lu et al.[199] Adapted with permission from ref 199. Copyright 2005 American Chemical Society.

to retain water instead of showing the burst-like behavior observed by Hummer et al.[98] and Waghe et al.[167] (see section 7.4). Ab initio calculations[197] on open-ended finite-length SWNTs suggest that, in this case, chirality can play a certain role. At the tube ends, in fact, a finite charge and dipole moment was observed in all the simulations, but, in the case of armchair nanotubes, the electrons are shared and less localized. Thus, in armchair nanotubes, the magnitude of the local charges is lower than in the case of zigzag nanotubes. In Won et al.[201] the effect of the aforementioned phenomenon on water transport in (6,6) and (10,0) SWNTs was investigated. In the case of two CNTs approximately 12 Å long, the partial charges at the ends of a (10,0) tube are around 4.5 times higher than those of a (6,6) tube (0.32e versus 0.07e). A consequence of this is that in the (10,0) tube, water dipoles point toward the walls resulting in the formation of L or D defects. This is not observed in the (6,6) tube where dipole vectors of all the water molecules inside the tube point toward the axis of the CNT. These examples highlight the importance of ab initio simulations in studying those properties that relate to the electronic structure and cannot be determined with the classical approach.

## 11. Selective Partitioning

A property of CNTs that it is strictly related to the water/CNT environment is the selective solute partitioning. There are some recent studies (e.g., methane by Kalra et al.,[202] ions in charged CNTs by Yang and Garde,[203] or RNA fragments by Yeh and Hummer[204]) that show how certain chemical species in aqueous solution can be spontaneously partitioned into nanotubes. The selectivity appears to emerge as a consequence of interplay of solute−water interactions in the bulk and solute−water−CNT interactions in the tube. Both methane and CNTs are, for instance, hydrophobic. As a consequence, the lower free energy is achieved when the methane molecules are inside the nanotube. When CNTs are placed in a water/methane solution, after a certain time (less than 1 ns), they begin to behave as "molecular straws" to selectively partition methane from the solution. Other examples show that not only is it possible to separate the solute from the solvent, but it is also possible to selectively extract specific solutes with respect to others in the same solution. In the case of $Na^+$, $K^+$, and $Cs^+$ cations in water solution,[203] for instance, negatively charged CNTs display selectivity toward the larger $K^+$ and $Cs^+$ cations over the smaller $Na^+$ ions.

This CNT property can have practical application in many separation and extraction processes, but it must not be confused with filtration, where the flow of ions or other chemical species through the membrane is hampered by steric hindrance and not by free energy considerations. In one of the previous examples,[202] on the other hand, the nanotube diameter was large enough to contain both methane and water, but the entrance of $H_2O$ molecules was thermodynamically disadvantageous with respect to the entrance of $CH_4$ molecules.

## 12. Functionalized Carbon Nanotubes

A way to influence the characteristics of water inside CNTs is represented by chemical functionalization. This is a very wide research area that, at the moment, mainly concerns the chemistry of CNTs.[205] In this section, we briefly mention only those articles that have a direct connection with water MD simulations.

Joseph et al.[206] studied ionic flow in CNTs functionalized by −COOH groups at both ends. Their results showed that selectivity between cations and anions can be obtained by these functional groups. Zheng et al.[138] anchored −COOH groups on the inner wall of a CNT to change its hydrophobic surface into hydrophilic and carried out simulations to study the transport of water and methanol mixtures through these functionalized carbon nanotubes (FCNTs). Halicioglu and Jaffe[207] found that the polar functional groups in water are energetically more stable, while nonpolar functional groups tend to remain folded. Huang et al.[208] carried out MD simulations to study the structural properties of water molecules confined in CNTs functionalized at their open ends with hydrophilic −COOH or hydrophobic $-CH_3$ groups. The same research group[156] studied the effect of helicity and temperature on the properties of water confined in −COOH FCNTs. It was found that the temperature has, in general, little effect. However, since the configuration of the −COOH groups at the open end of a CNT depends on helicity, this parameter can affect water diffusion inside CNTs. Striolo et al.,[141] finally, decorated the inner walls of SWNTs with carbonyl groups (C═O). Their results show that it is possible to a certain extent to manipulate the structure of water within CNTs by varying the concentration and the location of these groups.

These studies represent only the tip of the iceberg of the virtually endless possibilities represented by functionalized CNT. The main application of CNTs we considered in this review concerned the possibility of storing or transporting fluids within nanotubes. Functionalization adds a new perspective to both these cases. On the one hand, functional groups located at the entrance of the nanotube can act as selective gates that can open, allowing the transit of certain chemical species, and close, blocking the entrance to the others. On the other hand, functional groups can be added directly to the walls of the nanotube affecting opportunely the structure of the fluid stored in the CNT.

## 13. Conclusions

In this review, the recent advances in the area of molecular dynamics of water in carbon nanotubes are presented and discussed. We showed that many properties of water change under confinement and are strongly dependent on the nanotube size. There is, in particular, a neat discontinuity between the single-file structure in small nanotubes, where only a single molecular file of water is allowed, and the layered mode, where the molecules arrange themselves in concentric layers covering the internal walls of the nanotube. In a certain way, water inside nanotubes is a different substance from the water we experience in our everyday life. Even at room conditions, confined water shows ordered structures, which are characteristic of the solid state, but, at the same time, it conserves many properties of the liquid phase. Due to the effect of confinement, the phase diagram of water gains a new dimension (the nanotube diameter). However, the results available in the literature are scattered and they do not allow, at the moment, to map the entire three-dimensional phase diagram of water in CNTs. This task faces certain difficulties due to the necessity of finding an adequate water model. The fact is that all the water models available are parametrized for bulk water and we do not know how reliable they are in the case of confined water. Results obtained with different water models provide different pictures of the structure of the water layers. Experiments cannot always help because, at this scale, they also face certain difficulties and, moreover, there is also the possibility that a common water model for all the CNT sizes cannot be found within the classical approximation. From this prospective, ab initio simulations can represent the optimal answer since they are based on first principles and do not require any parametrized force field. These kinds of simulations, however, are much more expensive in terms of computational recourses and, at the moment, the only ab initio simulations available in the literature concern small nanotubes. This situation, at least for nanotubes of average size (10−15 Å), is likely to change relatively soon since the computational power affordable by the academic and research institutions is rapidly increasing. Different classical water models have, as discussed above, different outcomes in terms of water structures, but, when it comes to many water properties, they give relatively consistent results. For this reason, even though the theoretical objection that water models are not reliable in confined space still holds, in practice, classic molecular dynamics can be used to investigate CNT/water systems of practical interest.

## 14. Acknowledgments

This work has been performed under the UCY-CompSci project, a Marie Curie Transfer of Knowledge (TOK-DEV) grant (contract No. MTKD-CT-2004-014199) funded by the CEC under the sixth Framework Program.

## 15. References

(1) Monthioux, M.; Kuznetsov, V. L. *Carbon* **2006**, *44*, 1621.
(2) Hughes, T. V.; Chambers, C. R. US Patent 405480, 1889.
(3) Wei, J. Q.; Zhu, H. W.; Wu, D. H.; Wei, B. Q. *Appl. Phys. Lett.* **2004**, *84*, 4869.
(4) Pélabon, C.; Pélabon, H. *Acad. Sci. Paris* **1903**, *137*, 706.
(5) Schützenberger, P.; Schützenberger, L. *Acad. Sci. Paris* **1890**, *111*, 774.
(6) Radushkevich, L.; Lukyanovich, V. *Zh. Fis. Khim.* **1952**, *26*, 88.
(7) Iijima, S. *Nature* **1991**, *354*, 56.
(8) Iijima, S.; Ichihashi, T. *Nature* **1993**, *363*, 603.
(9) Bethune, D. S.; Kiang, C. H.; Devries, M. S.; Gorman, G.; Savoy, R.; Vazquez, J.; Beyers, R. *Nature* **1993**, *363*, 605.
(10) ThomsonScientific, "Web of Science (ISI)", http://portal.isiknowledge.com/portal.cgi, last visited 15 March 2008.
(11) Elsevier, "Scopus Citation Index", http://www.scopus.com, last visited 12 March 2008.
(12) Kuusi, O.; Meyer, M. *Scientometrics* **2007**, *70*, 759.
(13) Ajayan, P. M. *Chem. Rev.* **1999**, *99*, 1787.

(14) Dresselhaus, M.; Dresselhaus, G.; Eklund, P.; Saito, R. *Phys. World* **1998**, *11*, 33.
(15) Cao, D. P.; Zhang, X. R.; Chen, J. F.; Wang, W. C.; Yun, J. *J. Phys. Chem. B* **2003**, *107*, 13286.
(16) Liu, C.; Fan, Y. Y.; Liu, M.; Cong, H. T.; Cheng, H. M.; Dresselhaus, M. S. *Science* **1999**, *286*, 1127.
(17) Baughman, R. H.; Cui, C. X.; Zakhidov, A. A.; Iqbal, Z.; Barisci, J. N.; Spinks, G. M.; Wallace, G. G.; Mazzoldi, A.; De Rossi, D.; Rinzler, A. G.; Jaschinski, O.; Roth, S.; Kertesz, M. *Science* **1999**, *284*, 1340.
(18) Sazonova, V.; Yaish, Y.; Ustunel, H.; Roundy, D.; Arias, T. A.; McEuen, P. L. *Nature* **2004**, *431*, 284.
(19) Kong, J.; Franklin, N. R.; Zhou, C. W.; Chapline, M. G.; Peng, S.; Cho, K. J.; Dai, H. J. *Science* **2000**, *287*, 622.
(20) Snow, E. S.; Perkins, F. K.; Houser, E. J.; Badescu, S. C.; Reinecke, T. L. *Science* **2005**, *307*, 1942.
(21) Hinds, B. J.; Chopra, N.; Rantell, T.; rews, R.; Gavalas, V.; Bachas, L. G. *Science* **2004**, *303*, 62.
(22) Kalra, A.; Garde, S.; Hummer, G. *Proc. Natl. Acad. Sci. U.S.A.* **2003**, *100*, 10175.
(23) Hong, M. H.; Kim, K. H.; Bae, J.; Jhe, W. *Appl. Phys. Lett.* **2000**, *77*, 2604.
(24) Kim, P.; Lieber, C. M. *Science* **1999**, *286*, 2148.
(25) Baughman, R. H.; Zakhidov, A. A.; de Heer, W. A. *Science* **2002**, *297*, 787.
(26) Power, T. D.; Skoulidas, A. I.; Sholl, D. S. *J. Am. Chem. Soc.* **2002**, *124*, 1858.
(27) Portney, N. G.; Ozkan, M. *Anal. Bioanal. Chem.* **2006**, *384*, 620.
(28) Singh, R.; Pantarotto, D.; Lacerda, L.; Pastorin, G.; Klumpp, C.; Prato, M.; Bianco, A.; Kostarelos, K *Proc. Natl. Acad. Sci. U.S.A.* **2006**, *103*, 3357.
(29) Cherukuri, P.; Bachilo, S. M.; Litovsky, S. H.; Weisman, R. B. *J. Am. Chem. Soc.* **2004**, *126*, 15638.
(30) Kam, N. W. S.; Jessop, T. C.; Wender, P. A.; Dai, H. J. *J. Am. Chem. Soc.* **2004**, *126*, 6850.
(31) Porter, A.; Gass, M.; Muller, K.; Skepper, J.; Midgley, P.; Welland, M. *Nat. Nanotechnol.* **2007**, *2*, 713.
(32) Kam, N. W. S.; O'Connell, M.; Wisdom, J. A.; Dai, H. J. *Proc. Natl. Acad. Sci. U.S.A.* **2005**, *102*, 11600.
(33) Cheng, H. S.; Cooper, A. C.; Pez, G. P.; Kostov, M. K.; Piotrowski, P.; Stuart, S. J. *J. Phys. Chem. B* **2005**, *109*, 3780.
(34) Sansom, M. S. P.; Kerr, I. D.; Breed, J.; Sankararamakrishnan, R. *Biophys. J.* **1996**, *70*, 693.
(35) Sansom, M. S. P.; Biggin, P. C. *Nature* **2001**, *414*, 156.
(36) Floquet, N.; Coulomb, J. P.; Dufau, N.; re, G. *J. Phys. Chem. B* **2004**, *108*, 13107.
(37) Lu, D. Y.; Aksimentiev, A.; Shih, A. Y.; Cruz-Chu, E.; Freddolino, P. L.; Arkhipov, A.; Schulten, K. *Phys. Biol.* **2006**, *3*, 40.
(38) Gordillo, M. C.; Martí, J. *Chem. Phys. Lett.* **2000**, *329*, 341.
(39) Menke, H. *Phys. Z.* **1932**, *33*, 593.
(40) Prins, J. A. *Naturwissenschaften* **1931**, *19*, 435.
(41) Morrell, W. E.; Hildebrand, J. H. *J. Chem. Phys.* **1936**, *4*, 224.
(42) Fermi, E.; Pasta, J. *Studies in Non-Linear Problems*, Document L-1940 266, Los Alamos Report, 1955. Reprinted from the *American Mathematical Monthly*; Vol. 74, No. 1, Part I, Jan **1967**.
(43) Hullmann, A. *Scientometrics* **2007**, *70*, 739.
(44) Allen, M. P.; Tildesley, D. J. Computer Simulation of Liquids; Clarendon: London, 1987.
(45) Haile, J. M. *Molecular Dynamics Simulation: Elementary Methods*; Wiley-Interscience: New York, 1997.
(46) Frenkel, D.; Smit, B. *Understanding Molecular Simulation*, Academic Press: New York, 2001.
(47) Rapaport, D. C. *The Art of Molecular Dynamics Simulation*; Cambridge University Press: London, 2004.
(48) McCammon, J. A.; Harvey, S. C. *Dynamics of Proteins and Nucleic Acids*; Cambridge University Press: London, 1998.
(49) Pearlman, D. A.; Case, D. A.; Caldwell, J. W.; Ross, W. S.; Cheatham, T. E.; Debolt, S.; Ferguson, D.; Seibel, G.; Kollman, P. *Comput. Phys. Commun.* **1995**, *91*, 1.
(50) Van Der Spoel, D.; Lindahl, E.; Hess, B.; Groenhof, G.; Mark, A. E.; Berendsen, H. J. C. *J. Comput. Chem.* **2005**, *26*, 1701.
(51) Brooks, B. R.; Bruccoleri, R. E.; Olafson, B. D.; States, D. J.; Swaminathan, S.; Karplus, M. *J. Comput. Chem.* **1983**, *4*, 187.
(52) Jorgensen, W. L.; Maxwell, D. S.; TiradoRives, J. *J. Am. Chem. Soc.* **1996**, *118*, 11225.
(53) Allinger, N. L.; Yuh, Y. H.; Lii, J. H. *J. Am. Chem. Soc.* **1989**, *111*, 8551.
(54) Allinger, N. L.; Chen, K. S.; Lii, J. H. *J. Comput. Chem.* **1996**, *17*, 642.
(55) Mayo, S. L.; Olafson, B. D.; Goddard, W. A. *J. Phys. Chem.* **1990**, *94*, 8897.
(56) Piquemal, J. P.; Perera, L.; Cisneros, G. A.; Ren, P. Y.; Pedersen, L. G.; Darden, T. A. *J. Chem. Phys.* **2006**, *125*, 054511.
(57) Ponder, J. W.; Case, D. A. *Protein Simul.* **2003**, *66*, 27.
(58) Gao, H. J.; Kong, Y. *Annu. Rev. Mater. Res.* **2004**, *34*, 123.
(59) Lennard-Jones, J. E. *Proc. Phys. Soc.* **1931**, *43*, 461.
(60) Banerjee, S.; Murad, S.; Puri, I. K. *Chem. Phys. Lett.* **2007**, *434*, 292.
(61) Ewald, P. P. *Ann. Phys.* **1921**, *64*, 253.
(62) Darden, T.; York, D.; Pedersen, L. *J. Chem. Phys.* **1993**, *98*, 10089.
(63) Phillips, J. C.; Braun, R.; Wang, W.; Gumbart, J.; Tajkhorshid, E.; Villa, E.; Chipot, C.; Skeel, R. D.; Kale, L.; Schulten, K. *J. Comput. Chem.* **2005**, *26*, 1781.
(64) Martin, R. M. *Electronic Structures, Basic Theory and Practical Methods*; Cambridge University Press: London, 2004.
(65) Cook, D. B. *Handbook of Computational Quantum Chemistry*; Dover: New York, 2005.
(66) Kohanoff, J. *Electronic Structure Calculations for Solids and Molecules: Theory and Computational Methods*; Cambridge University Press: London, 2006.
(67) Berendsen, H. J. C.; Postma, J. P. M.; Vangunsteren, W. F.; Dinola, A.; Haak, J. R. *J. Chem. Phys.* **1984**, *81*, 3684.
(68) Nosé, S. *J. Chem. Phys.* **1984**, *81*, 511.
(69) Hoover, W. G. *Phys. Rev. A* **1985**, *31*, 1695.
(70) Parrinello, M.; Rahman, A. *J. Appl. Phys.* **1981**, *52*, 7182.
(71) Heo, S.; Sinnott, S. B. *J. Nanosci. Nanotechnol.* **2007**, *7*, 1518.
(72) Iijima, S.; Yudasaka, M.; Yamada, R.; Bandow, S.; Suenaga, K.; Kokai, F.; Takahashi, K. *Chem. Phys. Lett.* **1999**, *309*, 165.
(73) Yuan, L. M.; Saito, K.; Pan, C. X.; Williams, F. A.; Gordon, A. S. *Chem. Phys. Lett.* **2001**, *340*, 237.
(74) Yuan, L. M.; Saito, K.; Hu, W. C.; Chen, Z. *Chem. Phys. Lett.* **2001**, *346*, 23.
(75) Duan, H. M.; Mckinnon, J. T. *J. Phys. Chem.* **1994**, *98*, 12815.
(76) Murr, L. E.; Bang, J. J.; Esquivel, E. V.; Guerrero, P. A.; Lopez, A. *J. Nano. Res.* **2004**, *6*, 241.
(77) Ebbesen, T. W.; Ajayan, P. M. *Nature* **1992**, *358*, 220.
(78) Guo, T.; Nikolaev, P.; Thess, A.; Colbert, D. T.; Smalley, R. E. *Chem. Phys. Lett.* **1995**, *243*, 49.
(79) Joseyacaman, M.; Mikiyoshida, M.; Rendon, L.; Santiesteban, J. G. *Appl. Phys. Lett.* **1993**, *62*, 657.
(80) Rafii-Tabar, H. *Phys. Rep.* **2004**, *390*, 235.
(81) Reibold, M.; Paufler, P.; Levin, A. A.; Kochmann, W.; Patzke, N.; Meyer, D. C. *Nature* **2006**, *444*, 286.
(82) Charlier, A.; McRae, E.; Heyd, R.; Charlier, M. F.; Moretti, D. *Carbon* **1999**, *37*, 1779.
(83) Dresselhaus, M. S.; Dresselhaus, G.; Saito, R. Physics of Carbon Nanotubes. In *Carbon Nanotubes*; Endo, M., Iijima, S., Dresselhaus, M. S., Eds.; Pergamon: New York, 1996.
(84) Tsung-Lung, L.; Jyh-Hua, T. *Phys. B: Condens. Matter* **2007**, *393*, 195.
(85) Yao, Z. H.; Zhu, C. C.; Cheng, M.; Liu, J. H. *Comput. Mater. Sci.* **2001**, *22*, 180.
(86) Zhu, C. Z.; Guo, W.; Yu, T. X.; Woo, C. H. *Nanotechnology* **2005**, *16*, 1035.
(87) Belytschko, T.; Xiao, S. P.; Schatz, G. C.; Ruoff, R. S. *Phys. Rev. B* **2002**, *65*, 235430.
(88) Longhurst, M. J.; Quirke, N. *Mol. Simul.* **2005**, *31*, 135.
(89) Chen, M. J.; Liang, Y. C.; Li, H. Z.; Li, D. *Chin. Phys.* **2006**, *15*, 2676.
(90) Ruoff, R. S.; Qian, D.; Liu, W. K. C. R. *Phys.* **2003**, *4*, 993.
(91) Tersoff, J. *Phys. Rev. Lett.* **1986**, *56*, 632.
(92) Brenner, D. W. *Phys. Rev. B* **1990**, *42*, 9458.
(93) Huhtala, M.; Kuronen, A.; Kaski, K. *Comput. Phys. Commun.* **2002**, *146*, 30.
(94) Huhtala, M.; Kuronen, A.; Kaski, K. *Comput. Phys. Commun.* **2002**, *147*, 91.
(95) Garg, A.; Han, J.; Sinnott, S. B. *Phys. Rev. Lett.* **1998**, *81*, 2260.
(96) Garg, A.; Sinnott, S. B. *Chem. Phys. Lett.* **1998**, *295*, 273.
(97) Harrison, J. A.; Stuart, S. J.; Robertson, D. H.; White, C. T. *J. Phys. Chem. B* **1997**, *101*, 9682.
(98) Hummer, G.; Rasaiah, J. C.; Noworyta, J. P. *Nature* **2001**, *414*, 188.
(99) Zhou, X. Y.; Lu, H. J. *Chin. Phys.* **2007**, *16*, 335.
(100) Zou, J.; Ji, B. H.; Feng, X. Q.; Gao, H. J. *Small* **2006**, *2*, 1348.
(101) Longhurst, M. J.; Quirke, N. *Phys. Rev. Lett.* **2007**, *98*, 145503.
(102) Longhurst, M. J.; Quirke, N. *J. Chem. Phys.* **2006**, *124*, 234708.
(103) Longhurst, M. J.; Quirke, N. *J. Chem. Phys.* **2006**, *125*, 184705.
(104) Alexiadis, A.; Kassinos, S. *Chem. Eng. Sci.* **2008**, *63*, 2093.
(105) Alexiadis, A.; Kassinos, S. *Mol. Simul.* **2008**, *34*, 671.
(106) Andreev, S.; Reichman, D. R.; Hummer, G. *J. Chem. Phys.* **2005**, *123*, 194502.
(107) Chaplin, M. Water Structure and Bahavior;http://www.lsbu.ac.uk/water, last visited 16 May 2007.
(108) Guillot, B. *J. Mol. Liq.* **2002**, *101*, 219.
(109) Dellago, C.; Naor, M. M.; Hummer, G. *Phys. Rev. Lett.* **2003**, *90*, 105902.
(110) Mann, D. J.; Halls, M. D. *Phys. Rev. Lett.* **2003**, *90*, 195503.

(111) Teleman, O.; Jonsson, B.; Engstrom, S. *Mol. Phys.* **1987**, *60*, 193.
(112) Fanourgakis, G. S.; Xantheas, S. S. *J. Phys. Chem. A* **2006**, *110*, 4100.
(113) Kolesnikov, A. I.; Loong, C. K.; de Souza, N. R.; Burnham, C. J.; Moravsky, A. P. *Phys. B: Condens. Matter* **2006**, *385*, 272.
(114) Kolesnikov, A. I.; Zanotti, J. M.; Loong, C. K.; Thiyagarajan, P.; Moravsky, A. P.; Loutfy, R. O.; Burnham, C. J. *Phys. Rev. Lett.* **2004**, *93*, 035503.
(115) Walther, J. H.; Jaffe, R.; Halicioglu, T.; Koumoutsakos, P. *J. Phys. Chem. B* **2001**, *105*, 9980.
(116) Bojan, M. J.; Steele, W. A. *Langmuir* **1987**, *3*, 1123.
(117) Werder, T.; Walther, J. H.; Jaffe, R. L.; Halicioglu, T.; Koumoutsakos, P. *J. Phys. Chem. B* **2003**, *107*, 1345.
(118) Wang, J.; Zhu, Y.; Zhou, J.; Lu, X. H. *Phys. Chem. Chem. Phys.* **2004**, *6*, 829.
(119) Werder, T.; Walther, J.; Jaffe, R.; Koumoutsakos, P. Water-carbon interactions: Potential energy calibration using experimental data. In *2003 Nanotechnology Conference and Trade Show—Nanotech 2003*, San Francisco, CA, 2003; Vol. 3.
(120) Nijmeijer, M. J. P.; Bruin, C.; Bakker, A. F.; Vanleeuwen, J. M. J. *Phys. Rev. A* **1990**, *42*, 6052.
(121) Adamson, A. W.; Gast, A. P. *Physical Chemistry of Surfaces*, 6th ed.; John Wiley & Sons: New York, 1997.
(122) Rieutord, F.; Salmeron, M. *J. Phys. Chem. B* **1998**, *102*, 3941.
(123) Werder, T.; Walther, J. H.; Jaffe, R. L.; Halicioglu, T.; Noca, F.; Koumoutsakos, P. *Nano Lett.* **2001**, *1*, 697.
(124) Werder, T.; Walther, J.; Koumoutsakos, P. Hydrodynamics of carbon nanotubes—Contact angle and hydrophobic hydration. In *International Conference on Computational Nanoscience and Nanotechnology—ICCN 2002*, San Juan, 2002,
(125) Gogotsi, Y.; Libera, J. A.; Guvenc-Yazicioglu, A.; Megaridis, C. M. *Appl. Phys. Lett.* **2001**, *79*, 1021.
(126) Liu, H.; Zhai, J.; Jiang, L. *Soft Matter* **2006**, *2*, 811.
(127) Lau, K. K. S.; Bico, J.; Teo, K. B. K.; Chhowalla, M.; Amaratunga, G. A. J.; Milne, W. I.; McKinley, G. H.; Gleason, K. K. *Nano Lett.* **2003**, *3*, 1701.
(128) Barthlott, W.; Neinhuis, C. *Planta* **1997**, *202*, 1.
(129) Travis, K. P.; Todd, B. D.; Evans, D. J. *Phys. Rev. E* **1997**, *55*, 4288.
(130) Mao, Z. G.; Sinnott, S. B. *J. Phys. Chem. B* **2000**, *104*, 4618.
(131) Sokhan, V. P.; Nicholson, D.; Quirke, N. *J. Chem. Phys.* **2002**, *117*, 8531.
(132) Ackerman, D. M.; Skoulidas, A. I.; Sholl, D. S.; Johnson, J. K. *Mol. Simul.* **2003**, *29*, 677.
(133) Tuzun, R. E.; Noid, D. W.; Sumpter, B. G.; Merkle, R. C. *Nanotechnology* **1996**, *7*, 241.
(134) Abraham, F. F. *J. Chem. Phys.* **1978**, *68*, 3713.
(135) Bitsanis, I.; Magda, J. J.; Tirrell, M.; Davis, H. T. *J. Chem. Phys.* **1987**, *87*, 1733.
(136) Allen, T. W.; Kuyucak, S.; Chung, S. H. *J. Chem. Phys.* **1999**, *111*, 7985.
(137) Travis, K. P.; Gubbins, K. E. *J. Chem. Phys.* **2000**, *112*, 1984.
(138) Zheng, J.; Lennon, E. M.; Tsao, H. K.; Sheng, Y. J.; Jiang, S. Y. *J. Chem. Phys.* **2005**, *122*, 214702.
(139) Striolo, A.; Chialvo, A. A.; Gubbins, K. E.; Cummings, P. T. *J. Chem. Phys.* **2005**, *122*, 234712.
(140) Striolo, A. *Nano Lett.* **2006**, *6*, 633.
(141) Striolo, A.; Chialvo, A. A.; Cummings, P. T.; Gubbins, K. E. *J. Chem. Phys.* **2006**, *124*, 074710.
(142) Noon, W. H.; Ausman, K. D.; Smalley, R. E.; Ma, J. P. *Chem. Phys. Lett.* **2002**, *355*, 445.
(143) Liu, Y. C.; Wang, Q.; Wu, T.; Zhang, L. *J. Chem. Phys.* **2005**, *123*, 234701.
(144) Liu, Y. C.; Wang, Q.; Zhang, L.; Wu, T. *Langmuir* **2005**, *21*, 12025.
(145) Koga, K.; Gao, G. T.; Tanaka, H.; Zeng, X. C. *Nature* **2001**, *412*, 802.
(146) Mashl, R. J.; Joseph, S.; Aluru, N. R.; Jakobsson, E. *Nano Lett.* **2003**, *3*, 589.
(147) de Souza, N. R.; Kolesnikov, A. I.; Burnham, C. J.; Loong, C. K. *J. Phys.: Condens. Matter* **2006**, *18*, 2321.
(148) Takaiwa, D.; Koga, K.; Tanaka, H. *Mol. Simul.* **2007**, *33*, 127.
(149) Koga, K.; Gao, G. T.; Tanaka, H.; Zeng, X. C. *Physica A* **2002**, *314*, 462.
(150) Gay, S. C.; Smith, E. J.; Haymet, A. D. J. *J. Chem. Phys.* **2002**, *116*, 8876.
(151) Mamontov, E.; Burnham, C. J.; Chen, S. H.; Moravsky, A. P.; Loong, C. K.; de Souza, N. R.; Kolesnikov, A. I. *J. Chem. Phys.* **2006**, *124*, 194703.
(152) Maniwa, Y.; Kataura, H.; Abe, M.; Suzuki, S.; Achiba, Y.; Kira, H.; Matsuda, K. *J. Phys. Soc. Jpn.* **2002**, *71*, 2863.
(153) Matsuda, K.; Hibi, T.; Kadowaki, H.; Kataura, H.; Maniwa, Y. *Phys. Rev. B* **2006**, *74*, 073415.
(154) Vega, C.; Sanz, E.; Abascal, J. L. F. *J. Chem. Phys.* **2005**, *122*, 114507.
(155) Truskett, T. M. *Proc. Natl. Acad. Sci. U.S.A.* **2003**, *100*, 10139.
(156) Huang, L. L.; Shao, Q.; Lu, L. H.; Lu, X. H.; Zhang, L. Z.; Wang, J.; Jiang, S. Y. *Phys. Chem. Chem. Phys.* **2006**, *8*, 3836.
(157) Liu, Y. C.; Wang, Q. *Phys. Rev. B* **2005**, *72*, 085420.
(158) Liu, Y. C.; Wang, Q.; Li, X. F. *J. Chem. Phys.* **2005**, *122*, 044714.
(159) Martí, J.; Gordillo, M. C. *J. Chem. Phys.* **2001**, *114*, 10486.
(160) Alexiadis, A.; Kassinos, S. *Chem. Eng. Sci.* **2008**, *63*, 2047.
(161) Hanasaki, I.; Nakatani, A. *J. Chem. Phys.* **2006**, *124*, 144708.
(162) Hanasaki, I.; Nakatani, A. *J. Chem. Phys.* **2006**, *124*, 174714.
(163) Hanasaki, I.; Nakatani, A. *Modell. Simul. Mater. Sci. Eng.* **2006**, *14*, 9.
(164) Jorgensen, W. L.; Madura, J. D. *Mol. Phys.* **1985**, *56*, 1381.
(165) Zielkiewicz, J. *J. Chem. Phys.* **2005**, *123*, 104501.
(166) Luzar, A.; Chandler, D. *Nature* **1996**, *379*, 55.
(167) Waghe, A.; Rasaiah, J. C.; Hummer, G. *J. Chem. Phys.* **2002**, *117*, 10789.
(168) Dellago, C.; Naor, M. M. *Comput. Phys. Commun.* **2005**, *169*, 36.
(169) Marx, D.; Tuckerman, M. E.; Hutter, J.; Parrinello, M. *Nature* **1999**, *397*, 601.
(170) de Grotthuss, C. J. T. *Ann. Chim.* **1806**, *58*, 54.
(171) Tajkhorshid, E.; Nollert, P.; Jensen, M. O.; Miercke, L. J. W.; O'Connell, J.; Stroud, R. M.; Schulten, K. *Science* **2002**, *296*, 525.
(172) Zhu, F. Q.; Schulten, K. *Biophys. J.* **2003**, *85*, 236.
(173) Zimmerli, U.; Gonnet, P. G.; Walther, J. H.; Koumoutsakos, P. *Nano Lett.* **2005**, *5*, 1017.
(174) Rasaiah, J. C.; Garde, S.; Hummer, G. *Annu. Rev. Phys. Chem.* **2008**, *59*, 713.
(175) Berezhkovskii, A.; Hummer, G. *Phys. Rev. Lett.* **2002**, *89*, 064503.
(176) Holt, J. K.; Park, H. G.; Wang, Y. M.; Stadermann, M.; Artyukhin, A. B.; Grigoropoulos, C. P.; Noy, A.; Bakajin, O. *Science* **2006**, *312*, 1034.
(177) Einstein, A. *Ann. Phys.* **1906**, *19*, 289.
(178) Green, M. S. *J. Chem. Phys.* **1954**, *22*, 398.
(179) Harris, T. E. *J. Appl. Probability* **1965**, *2*, 323.
(180) Richards, P. M. *Phys. Rev. B* **1977**, *16*, 1393.
(181) Lee, K.; Sinnott, S. B. *Nano Lett.* **2005**, *5*, 793.
(182) Bao, J.-D.; Zhuo, Y.; Oliveira, F.; Hanggi, P. *Phys. Rev. E* **2006**, 74.
(183) Mukherjee, B.; Maiti, P. K.; Dasgupta, C.; Sood, A. K. *J. Chem. Phys.* **2007**, *126*, 1.
(184) Levitt, M.; Hirshberg, M.; Sharon, R.; Laidig, K. E.; Daggett, V. *J. Phys. Chem. B* **1997**, *101*, 5051.
(185) Wu, Y. J.; Tepper, H. L.; Voth, G. A. *J. Chem. Phys.* **2006**, *124*, 024503.
(186) Koplik, J.; Banavar, J. R. *Annu. Rev. Fluid Mech.* **1995**, *27*, 257.
(187) Heffelfinger, G. S.; Vanswol, F. *J. Chem. Phys.* **1994**, *100*, 7548.
(188) Kassinos, S. C.; Walther, J. H.; Kotsalis, E.; Koumoutsakos, P. *Lecture Notes in Computer Science*; Springer: New York, 2004; Vol. 39.
(189) Kotsalis, E. M.; Walther, J. H.; Koumoutsakos, P. *Int. J. Multiphase Flow* **2004**, *30*, 995.
(190) Sun, M.; Ebner, C. *Phys. Rev. A* **1992**, *46*, 4813.
(191) Li, J.; Liao, D. Y.; Yip, S. *Phys. Rev. E* **1998**, *57*, 7259.
(192) Huang, B. D.; Xia, Y. Y.; Zhao, M. W.; Li, F.; Liu, X. D.; Ji, Y. J.; Song, C. *J. Chem. Phys.* **2005**, *122*, 084708.
(193) Valentini, L.; Armentano, I.; Kenny, J. M. *Diamond Relat. Mater.* **2005**, *14*, 121.
(194) Benedict, L. X.; Louie, S. G.; Cohen, M. L. *Phys. Rev. B* **1995**, *52*, 8541.
(195) Dumitrica, T.; Landis, C. M.; Yakobson, B. I. *Chem. Phys. Lett.* **2002**, *360*, 182.
(196) Guo, G. Y.; Chu, K. C.; Wang, D. S.; Duan, C. G. *Comput. Mater. Sci.* **2004**, *30*, 269.
(197) Hou, S. M.; Shen, Z. Y.; Zhao, X. Y.; Xue, Z. Q. *Chem. Phys. Lett.* **2003**, *373*, 308.
(198) Arab, M.; Picaud, F.; Devel, M.; Ramseyer, C.; Girardet, C. *Phys. Rev. B* **2004**, *69*, 165401.
(199) Lu, D. Y.; Li, Y.; Ravaioli, U.; Schulten, K. *J. Phys. Chem. B* **2005**, *109*, 11461.
(200) Moulin, F.; Devel, M.; Picaud, S. *Phys. Rev. B* **2005**, *71*, 165401.
(201) Won, C. Y.; Joseph, S.; Aluru, N. R. *J. Chem. Phys.* **2006**, *125*, 114701.
(202) Kalra, A.; Hummer, G.; Garde, S. *J. Phys. Chem. B* **2004**, *108*, 544.
(203) Yang, L.; Garde, S. *J. Chem. Phys.* **2007**, *126*, 084706.
(204) Yeh, I. C.; Hummer, G. *Proc. Natl. Acad. Sci. U.S.A.* **2004**, *101*, 12177.
(205) Tasis, D.; Tagmatarchis, N.; Bianco, A.; Prato, M. *Chem. Rev.* **2006**, *106*, 1105.
(206) Joseph, S.; Mashl, R. J.; Jakobsson, E.; Aluru, N. R. *Nano Lett.* **2003**, *3*, 1399.
(207) Halicioglu, T.; Jaffe, R. L. *Nano Lett.* **2002**, *2*, 573.
(208) Huang, L. L.; Zhang, L. Z.; Shao, Q.; Wang, J.; Lu, L. H.; Lu, X. H.; Jiang, S. Y.; Shen, W. F. *J. Phys. Chem. B* **2006**, *110*, 25761.

(209) Berendsen, H. J. C.; Postma, J. P. M.; van Gunsteren, W. F.; Hermans, J. *Intermolecular Forces*; Reidel: Dordrecht, 1981.
(210) Berendsen, H. J. C.; Grigera, J. R.; Straatsma, T. P. *J. Phys. Chem.* **1987**, *91*, 6269.
(211) Jorgensen, W. L.; Chandrasekhar, J.; Madura, J. D.; Impey, R. W.; Klein, M. L. *J. Chem. Phys.* **1983**, *79*, 926.
(212) Mahoney, M. W.; Jorgensen, W. L. *J. Chem. Phys.* **2000**, *112*, 8910.
(213) Kiyohara, K.; Gubbins, K. E.; Panagiotopoulos, A. Z. *Mol. Phys.* **1998**, *94*, 803.
(214) van der Spoel, D.; van Maaren, P. J.; Berendsen, H. J. C. *J. Chem. Phys.* **1998**, *108*, 10220.
(215) Mahoney, M. W.; Jorgensen, W. L. *J. Chem. Phys.* **2001**, *114*, 363.
(216) Vega, C.; Abascal, J. L. F. *J. Chem. Phys.* **2005**, *123*, 144504.
(217) Yu, H. B.; van Gunsteren, W. F. *J. Chem. Phys.* **2004**, *121*, 9549.
(218) Kusalik, P. G.; Svishchev, I. M. *Science* **1994**, *265*, 1219.
(219) Baez, L. A.; Clancy, P. *J. Chem. Phys.* **1994**, *101*, 9837.
(220) Gubskaya, A. V.; Kusalik, P. G. *J. Chem. Phys.* **2002**, *117*, 5290.
(221) Stan, G.; Cole, M. W. *Surf. Sci.* **1998**, *395*, 280.
(222) Steele, W. A. *Interaction of Gases with Solid Surfaces*; Pergamon: Oxford, UK, 1974.
(223) Huang, B. D.; Xia, Y. Y.; Zhao, M. W.; Li, F.; Liu, X. D.; Ji, Y. J.; Song, C.; Tan, Z. Y.; Liu, H. *Chin. Phys. Lett.* **2004**, *21*, 2388.
(224) Wan, R. Z.; Li, J. Y.; Lu, H. J.; Fang, H. P. *J. Am. Chem. Soc.* **2005**, *127*, 7166.
(225) Kotsalis, E. M.; Demosthenous, E.; Walther, J. H.; Kassinos, S. C.; Koumoutsakos, P. *Chem. Phys. Lett.* **2005**, *412*, 250.
(226) Li, L. W.; Bedrov, D.; Smith, G. D. *J. Phys. Chem. B* **2006**, *110*, 10509.
(227) Hanasaki, I.; Nakatani, A. *Adv. Struct. Funct. Mater. Des. Process.* **2006**, *512*, 399.
(228) Xie, Y.; Kong, Y.; Gao, H.; Soh, A. *Comput. Mater. Sci.* **2007**, *40*, 460.

CR078140F